QSAR Studies on Blood-Brain Barrier Permeation

Juan M. Luco[1,*] and Eduardo Marchevsky[2]

[1]*Laboratorio de Alimentos,* [2]*Area de Química Analítica, Departamento de Química, Facultad de Química, Bioquímica y Farmacia, Universidad Nacional de San Luis, Chacabuco y Pedernera, 5700 San Luis, Argentina*

Abstract: This review focuses on both physicochemical and theoretical QSAR methods for the prediction of drug transport across the blood-brain barrier (BBB). Special emphasis is given to the recent progress that has been made in the modeling of BBB penetration, with a particular focus on the models based on kinetic parameters of BBB permeability dataset. Physicochemical models based on partition coefficients and chromatographic capacity factors, as well as computerized parameters such as polar surface area and hydrogen-bonding descriptors are described and their success and limitations are discussed. Theoretical models based on topological or molecular orbital calculations are summarized and assessed in terms of descriptors, model type, predictive performance and interpretability. Strengths and weaknesses of the various methods are described. Related issues that are mentioned include the transporter-mediated permeation of drugs across the BBB and its implications on the stability and predictive quality of QSAR models.

1. INTRODUCTION

Drug research is a multi-disciplinary process united by a common goal, which is the development of novel therapeutic agents. Drug research involves two separate stages: discovery/design and development. The former consists of the identification and characterization of macromolecular targets, synthesis and screening of new lead molecules for *in vitro* and/or *in vivo* biological activities, and assessing pharmacokinetic (PK) profiles of lead compounds. On the other hand, in the development stage, efforts are focused on the evaluation of *in vivo* ADME (absorption, distribution, metabolism and excretion) profile as well as toxicity factors of new drug candidates [1].

Pharmacokinetic/metabolism investigations are critical in all phases of a fully integrated drug development program. However, since the major reasons for failure in the development stage often involve inappropriate PK properties of lead compounds, the importance of including an ADME characterization of potential drug candidates as part of screening process it is now widely recognized by most pharmaceutical companies [2-5].

Quantitative structure-activity relationships (QSAR) represent one of the most effective computational approaches in the drug design process. Thus, QSAR has been successfully utilized in the design of bioactive compounds; some of them have been commercialized, and others are soon to be commercialized [6]. Since the early 1970s, significant efforts have been made toward developing QSAR models for the prediction of diverse pharmacokinetic properties. Thus, an extensive body of work has been published using quantitative structure-pharmacokinetics relationships, including absorption, distribution, protein binding, elimination, and metabolism of drugs. Several comprehensive reviews are available offering differing perspectives on this topic [7-17].

*Address correspondence to this author at the Laboratorio de Alimentos, Universidad Nacional de San Luis, Chacabuco y Pedernera, 5700 San Luis, Argentina; Fax: +54-2652-430224; E-mail: jmluco@unsl.edu.ar

Brain drug development requires advances in both brain drug discovery and brain drug delivery (see two recent reviews [57, 65]). Due to the presence of the blood-brain barrier (BBB), only small uncharged molecules (e.g., H_2O, CO_2) and moderately lipophilic compounds can cross the BBB barrier by passive diffusion. On the other hand, essential nutrients or otherwise hydrophilic molecules are transported into the brain by means of carrier-mediated processes. Therefore, to maximize the delivery of therapeutic compounds into the brain, it is essential to understand the factors governing blood-brain barrier permeability for developing safer and more effective CNS active drugs [18].

In recent years, several important reviews have been published on the prediction of BBB permeation by computational methods [19-22, 29-31]. The reader is referred to these works for detailed information. The aim of the present article is to review, as comprehensibly as possible, all QSAR studies made so far on drug transport across the blood-brain barrier. The review focuses on both physicochemical and theoretical QSAR models, with particular attention to the models based on kinetic parameters of BBB permeability dataset. Finally, related issues that are also discussed include the transporter-mediated permeation of drugs across the BBB and its implications on the stability and predictive quality of the QSAR models developed.

2. THE BLOOD-BRAIN BARRIER

The BBB is formed by characteristic tissue structures such as a continuous cellular layer of endothelial cells (EC) that are sealed by the presence of complex tight junctions, few pinocytic vesicles, and the absence of transport pores which restrict the intercellular transport of the substances. Under these conditions, most drugs enter into the brain by passive diffusion through the brain capillary endothelial cells, whereas essential nutrients or otherwise hydrophilic substances are transported into the brain by means of saturable, carrier-mediated transport mechanisms. The structural and functional aspects of the BBB have been recently reviewed by Begley and Brightman [27].

1573-4099/06 $50.00+.00 © 2006 Bentham Science Publishers Ltd.

Several transport systems have been identified in the endothelial cells that form the BBB, which are of great importance for the maintenance of a constant environment of the brain and for its optimal functioning. A sodium-independent stereospecific glucose carrier system (GLUT-1) has been characterized as transporting several sugars or sugar-analogues with high capacity. Six high affinity amino acid carrier systems have been described for large neutral amino acids (LNAA system), for basic amino acids (y^+ system), for acidic amino acids (X^- system) and for neutral and/or cationic amino acids (A, B^{0+}, and ASC systems), respectively. Furthermore, carrier systems for monocarboxylic acids (MCT), nucleosides (NT), amines (choline transporter) and peptides have been identified. To this end, four major families of organic ion transporters have been described: organic anion transporters (OATs), organic cation transporters (OCTs), organic anion transporter proteins (OATPs), and the organic cation/carnitine transporters (OCTNs). For a detailed discussion about the transport systems at BBB, the reader is referred to five recent reviews [23-25, 32-33].

In addition to these BBB transport systems, some of which operate equally well in both blood-to-brain and brain-to-blood directions, the BBB endothelial cells express a variety of metabolic enzymes, which are implicated in drug oxidation and conjugation, and membrane efflux systems (ABC-transporters), such as P-glycoprotein (P-gp), the multidrug-resistance proteins (MRPs) and the breast cancer resistance protein (BCRP). Furthermore, the presence of these efflux systems restricts the accumulation of many hydrophobic drugs in the CNS and, therefore, plays a predominant role in the bioavailability of several therapeutic compounds, such as several anticancer agents [26]. An excellent review on the ABC-transporters and their role in BBB has been recently published by Begley [28]. Moreover, it should be noted that MCT and OATs transport systems have also been implicated in the efflux of several drugs from the brain [23, 24].

In conclusion, the multiple functions of BBB make this a quite complex barrier that drugs must overcome to reach the brain parenchyma. A schematic representation of the various transporters involved in BBB permeability is presented in Fig. (**1**).

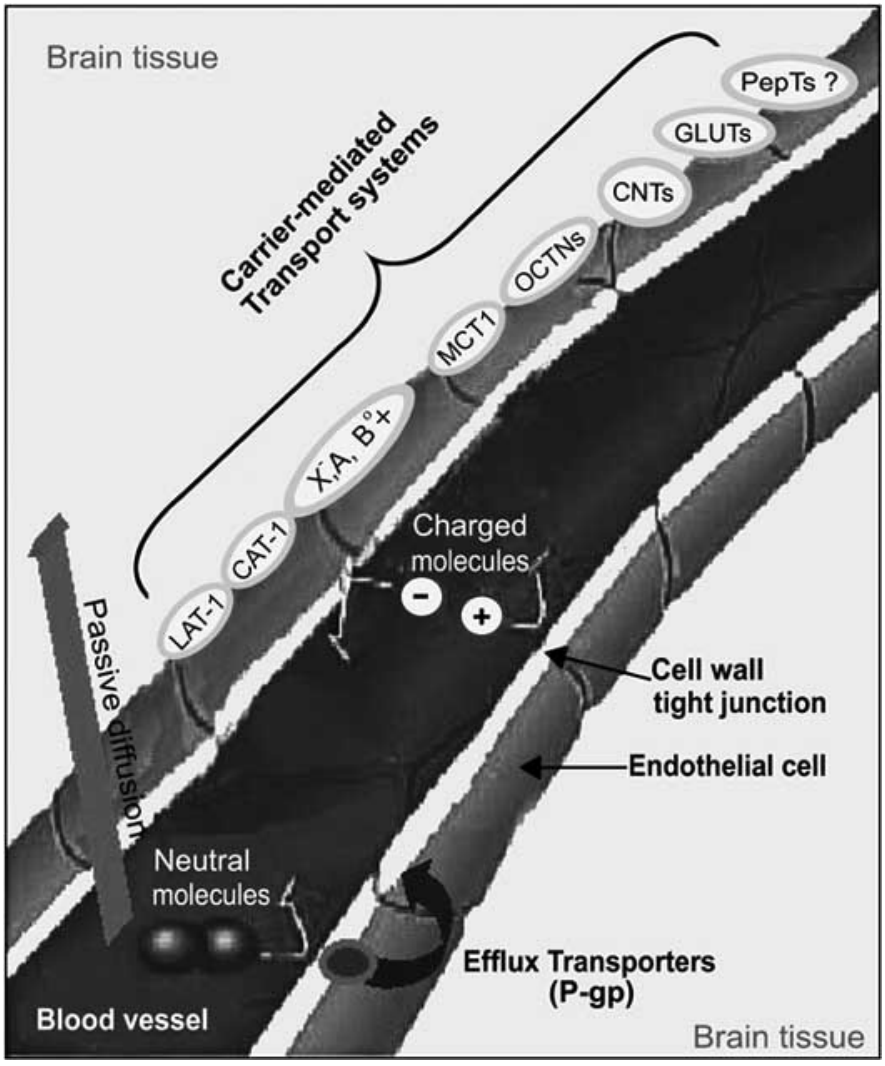

Fig (1). Schematic diagram of the blood-brain barrier and the carrier-mediated transport systems. Redrawn and modified from Ref. [161].

3. BIOLOGICAL METHODS USED IN BBB TRANSPORT STUDIES

Many *in vivo* and *in vitro* techniques have been developed to assess the rate, extent and mechanism of BBB permeability. Some of the methods more commonly used for studying transport across the BBB are briefly discussed below.

3.1 *In Vivo* BBB Models

The *in vivo* methods can be broadly classified according to two methodological approaches: (*i*) methods based on equilibrium studies between brain and blood, and (*ii*) methods based on kinetic parameters (e.g. permeability coefficient across the BBB) such as the single-pass techniques (e.g. brain uptake index (BUI) and the internal carotid artery infusion technique), the multiple-pass techniques (e.g. intravenous administration and *in situ* brain perfusion), and the intracerebral microdialysis technique.

In the former approach, a radiolabeled compound is administered intravenously and then, when the steady-state conditions are reached (2-3 hours later or until radioactivity in the blood reaches a plateau), the animal is sacrificed for collection and sampling of brain tissue and blood. The results are expressed as a concentration ratio defined through eq **1**:

$$BB = [\text{concentration in brain}] / [\text{concentration in blood}] \quad (1)$$

As will be reviewed later, the majority of the QSAR models developed for the prediction of BBB permeability have been based on this parameter. However, as recently stated by several authors [34-36], the BB parameter is not an appropriate index of BBB permeability since other factors apart from capillary permeability influence the final concentration of drug in the brain. This composite parameter is indeed a volume of distribution that represents the partitioning of drugs between the whole brain and the blood, and therefore, it is affected not only by the drug permeability at the BBB, but also by the rates of drug metabolism/excretion, binding of the drug to plasma proteins (mostly to albumin and α-acid glycoprotein) relative to the proteins and interstitial fluid of brain, and by the ratio of uncharged /charged drug present in the physiological environment. In addition, the drug-receptor interaction is a function of the free drug amount present in the brain cells and not of the total drug concentration, which is indeed reflected by log (BB).

On the other hand, the techniques based on permeation rates across the BBB give more useful measures on BBB permeability due to the fact that they can predict the level of free drug in the brain. Further, according to Pardridge [36], the only methodology that does give reliable measures of BBB permeability is the *in vivo* quantification of the BBB permeability-surface area (PS) product. Among different experimental approaches for quantifying the BBB permeability, the brain uptake index (BUI) is the most straightforward technique for examining CNS uptake. This approach involves the intracarotid injection (< 0.5 s) of a small bolus containing a ^{14}C-labeled test-compound and a ^{3}H-reference compound or vice versa. Afterwards, the animal is decapitated at a time post-injection fixed (5-15 s) for analysis of the radioactivity in the brain as well as in the injected solution (in-mix) into the carotid artery. The BUI index is calculated as:

$$BUI / (100\%) = \frac{([^{14}C \text{ test-compound}] / [^{3}H \text{ reference-compound}])_{\text{brain}}}{([^{14}C \text{ test-compound}] / [^{3}H \text{ reference-compound}])_{\text{in mix}}} = E_t / E_r \quad (2)$$

where E_t is the unidirectional extraction of the test compound and E_r the extraction of the reference compound. From the BUI index, the derivation of permeability surface (PS) area product is possible by means of Renkin-Crone equation [37]. The internal carotid artery infusion technique is a variant of BUI, although the time of injection is more than one second (15-60 s) and therefore, it is a more sensitive technique. The advantage of both techniques is that there is no systemic exposure of the test compound prior to transport across BBB and thus, there is no interference of its metabolites. On the other hand, the *in situ* brain perfusion technique offers several advantages over previously mentioned methods. Since this is not a single-pass technique, its sensitivity is substantially higher than those for the other methods, and therefore, it is more appropriate for drug screening that have a poor BBB permeability. In addition, this approach allows identification of compounds that are transported by both passive and carrier-mediated transport mechanisms. According to the pharmacokinetic rule, the concentration in brain tissue at a given time (t) depends on the PS product and on the area under the plasma concentration curve (AUC) according to the following equation: $\%ID/g_{(t)} = PS \times AUC_{0\text{-}t}$, where %ID/g = % injected dose per gram brain tissue. The BBB PS product ($\mu l\ min^{-1}\ g^{-1}$) is generally calculated as:

$$PS = \frac{[V_d - V_o]\ Cp\ (t)}{AUC} \quad (3)$$

where V_d is the brain volume of distribution of the test compound, V_o is the plasma volume of distribution of the marker, Cp (t) is the terminal plasma concentration, and AUC is the plasma area under the curve at a given time after administration. Several of the *in vivo* methods commonly utilized to examine drug transport through the BBB have been reviewed by Fenstermacher *et al.* [38] and Pardridge [42]. On the other hand intracerebral microdialysis is a sophisticated technique that offers several advantages in the BBB permeability studies. The most important issues are: (*i*) it is possible to obtain free drug concentration measurements within discrete brain regions; and (*ii*) numerous concentration-time data can be obtained from a single animal, which reduces the number of animals required for pharmacokinetic investigations. A series of extensive reviews on the use of microdialysis in drug delivery studies have been reported recently [39-41].

3.2 *In Vitro* Models

This review is not intended to be a comprehensive listing of all reports of *in vitro* methods used to study the permeation of drugs across to the BBB. The papers cited are intended to give a survey of progresses and limitations of these approaches in the BBB permeability studies.

As previously discussed, the *in vivo* methodologies based on permeation rates across the BBB are the unique ones that give reliable measures of the BBB permeability [36]. However, since animal-based assays are expensive, time-consuming and often require radiolabeled compounds, the need for appropriate estimation approaches, either by means of *in vitro* models or by using *in silico* prediction models, is a question of great importance for the pharmaceutical industry. Thus, as an alternative to the *in vivo* studies, several *in vitro* models have been developed in order to evaluate brain permeation as well as to identify the potential influx or efflux transport mechanisms at BBB of potential drug candidates. Among the *in vitro* techniques more commonly used in BBB permeability studies, those based on primary or passaged cultures of brain microvessel endothelial cells (BMEC) have received the greatest attention [43,45]. There are, however, many differences between *in vitro* BBB models and *in vivo* BBB transport systems. For instance, the bovine brain microvessel endothelial cells (BBMEC) isolated and grown on porous supports may form tight intercellular junctions from 6-14 days in culture. However, these BBMEC monolayers show a trans-endothelial electrical resistance (TEER) several-fold reduced relative to the *in vivo* TEER values and consequently, the *in vitro* paracellular transport is higher that the *in vivo* one. On the other hand, co-cultures of the above mentioned system with astrocytes or astrocyte-conditioned medium exhibit monolayers with tight junctions of major complexity and better developed, although, once more, the TEER values are not as high as those of *in vivo* models [44]. Moreover, it has been demonstrated that the gene expression of many BBB transporters is significantly downregulated in cultured cells [42]. Thus, while much work has been focused on ways of producing a better model of the BBB *in vitro*, according to Terasaki *et al.* [46], the *in vivo* BBB permeability cannot still be accurately predicted from the results obtained with primary or immortalized BMEC cultures.

This view is consistent with the results obtained from several comparative studies between both *in vivo* and *in vitro* BBB permeability data, which provide evidence that none of the commonly used *in vitro* models fully expresses the

Table 1. ***In vivo*** **and** ***in vitro*** **Permeability Data for Compounds Studied by Garberg** ***et al.*** **[47]**

Compound	Transport	M_W	LogDpH7.4	logP app (cm/s)[a]	logP e (cm/s)[b]	logP e (cm/s)[c]	logp e (cm/s)[d]
Alanine	Influx	89.10	-3.20	-5.018	-4.680	-4.364	-5.000
Antipyrine	Diffusion	188.20	0.11	-4.956	-3.506	-4.000	-4.640
AZT	Efflux	267.30	-0.58	-5.301	-5.187	nr	-4.750
Caffeine	Diffusion	194.20	-0.10	-5.092	-3.003	-4.312	-4.928
Cimetidine	Eflux	252.30	-0.40	-6.268	-5.367	-4.222	-5.187
Cyclosporine	Eflux	1202.60	5.00	-5.523	-5.155	-5.658	-5.824
Diazepam	Diffusion	284.80	2.10	-4.362	-3.480	nr	-4.462
Digoxin	Efflux	780.90	2.20	-6.699	-5.456	-5.824	-5.602
L-dopa	Influx	197.20	-2.70	-5.409	-4.681	-4.523	-4.783
Glycerol	Diffusion	92.10	-1.90	-5.125	-5.137	-4.398	-4.633
Inuin (^{3}H)	Diffusion	5000	-3.00	-8.292	-6.174	-4.903	-5.276
Lactic acid	Influx	90.10	-4.80	-4.730	-4.979	-3.611	-4.810
Leucine	Influx	131.20	-1.90	-4.836	-4.818	-3.987	-4.607
Morphine	Eflux	285.30	-0.44	-6.097	-4.642	nr	-4.664
Nicotine	Diffusion	162.20	-0.10	-5.208	-3.009	-4.573	-4.462
Phenytoin	Diffusion	152.30	2.50	-4.827	-3.910	-5.174	-4.695
Sucrose	Diffusion	342.30	-3.70	-6.495	-5.398	-4.573	-5.066
Urea	Diffusion	60.10	-1.60	-5.921	-4.432	-3.699	-4.411
Verapamil	Efflux	454.60	3.40	-5.201	-4.538	-4.398	-5.013
Vinblastine	Efflux	909.10	4.10	-5.796	-4.703	-4.523	-5.699
Vincristine	Efflux	923.00	0.45	-5.699	-5.602	-5.638	-5.174
Warfarin	Diffusion	308.30	0.90	-6.1.25	-4.542	-4.602	-5.481

(a)The apparent permeability coefficients obtained *in vivo* by mouse brain uptake assay (MBUA). (b) The endothelial permeability coefficients BBEC co-cultured with rat astrocytes, obtained from transport in the apical to basolateral direction (a>b). (c) The endothelial permeability coefficients from human primary brain endothelial cells (HPBEC) for (a>b) transport. (d) The endothelial permeability coefficients from SV40 immortalized rat brain endothelial cells (SV-ARBEC) for (a>b) transport.

(Table 1)contd.....

Compound	Transport	$LogP_{app}$(cm/s)[e]	$logP_{app}$ (cm/s)[f]	$logP_{app}$ (cm/s)[g]	$logP_{app}$ (cm/s)[h]	$logp_{app}$ (cm/s)[i]
Alanine	Influx	-4.316	-5.699	-5.194	-5.658	-5.432
Antipyrine	Diffusion	-4.101	-4.361	-4.275	-4.275	-4.370
AZT	Efflux	nr	-5.620	-5.237	-5.495	-4.967
Caffeine	Diffusion	nr	-4.400	-4.249	-4.272	-4.365
Cimetidine	Eflux	-4.393	-6.097	-5.824	-6.041	-6.097
Cyclosporine	Eflux	nr	-5.959	-5.420	-6.699	-6.155
Diazepam	Diffusion	-3.793	-4.426	-4.225	-4.280	-4.386
Digoxin	Efflux	-4.390	-6.097	-5.721	-6.215	-6.000
L-dopa	Influx	nr	-6.155	-5.432	-5.678	-6.000
Glycerol	Diffusion	nr	-6.222	-5.569	-5.678	-4.833
Inuin (^{3}H)	Diffusion	-4.648	-7.000	-6.678	-6.770	-7.523
Lactic acid	Influx	-4.342	-5.509	-5.114	-5.523	-6.000
Leucine	Influx	-4.373	-5.721	-5.194	-5.252	-4.812
Morphine	Eflux	nr	-5.658	-5.319	-5.367	-5.081
Nicotine	Diffusion	nr	-4.527	-4.268	-4.280	-4.545
Phenytoin	Diffusion	nr	-4.466	-4.320	-4.350	-4.398
Sucrose	Diffusion	nr	-6.699	-6.337	-6.481	-5.854
Urea	Diffusion	-4.061	-5.921	-5.569	-5.538	-5.229
Verapamil	Efflux	nr	-4.854	-4.386	-4.412	-4.804
Vinblastine	Efflux	-4.447	-5.886	-6.000	-6.469	-5.678
Vincristine	Efflux	nr	-6.699	-6.444	-6.367	-7.000
Warfarin	Diffusion	nr	-4.693	-4.523	-4.810	-4.495

(e)The apparent permeability coefficients from immortalized mouse brain endothelial cells (MBEC4) for (a>b) transport. (f) The apparent permeability coefficients form Madin-Darby canine kidney (MDCKATCC) cells for (a>b) transport. (g) The apparent permeability coefficients from Madin-Darby canine kidney (MDCKWT) cells for (a>b) transport. (h) The apparent permeability coefficients from Madin-Darby canine kidney (MDCKmdr-1) cells for (a>b) transport. (i) The apparent permeability coefficients from Caco-2 cells for (a>b) transport. Note: nr = reported in the original publication.

unique features of *in vivo* BBB transport. Perhaps the most comprehensive study on this topic corresponds to a work published very recently by Garberg *et al.* [47]. They studied the BBB penetration of twenty two compounds using two different *in vivo* models (mouse brain uptake assay and microdialysis) and several *in vitro* models based on nine cell lines such as BBMEC co-cultured with astrocytes, two immortalized brain endothelial cell lines (from rat and mouse), and five cell lines not derived from the BBB (ECV-C6, MDKCs and Caco-2). The main goal of this study was to find an *in vitro* model that could predict the *in vivo* transport of compounds across the BBB. The broad range of physicochemical properties, as well as different degrees of permeability of the studied compounds, can be observed in Table **1**. As evidenced from the correlation matrix shown in Table **2**, when the twenty two compounds were included in the analysis, no reasonable linear correlation was found between *in vivo* and *in vitro* permeability data for any of the screened *in vitro* models. Higher correlations, however, were found when only passively transported compounds were included in the analysis: bovine brain endothelial cells (r=0.86), $MDCK_{wt}$ (r = 0.81) and Caco-2 (r = 0.93). Additionally, active influx was not predicted by any of the assessed *in vitro* models and from a qualitative point of view, that is to say, from the plots of log P_{aap} *vs.* log $D_{pH7.4}$, the MDCKmdr-1 system was identified by the authors as the best model for distinguishing between compounds distributed by active efflux and those distributed by passive mechanisms.

A similar conclusion has also been reached by Pardridge *et al.* [48] by using *in vivo* and *in- vitro* BBB permeability data for 15 radiolabeled drugs reflecting different degrees of lipophilicity. The *in vitro* model was based on primary cultures of BBMEC, while the BBB PS products were obtained by using the internal carotid artery perfusion method in anesthetized rats. The reported correlation was as follows:

$$\ln (Pe_{(in\ vivo)} \times \sqrt{Mw}\ ) = -2.90 + 2.2 \ln (Pe_{(in\ vitro)} \times \sqrt{Mw}\ ) \quad (4)$$

$r^2 = 0.72$ r = 0.85 n = 13 ($p < 0.0005$)

In this equation, r^2 is the squared correlation coefficient, r is the correlation coefficient, and n is the number of compounds. The PS products were converted into endothelial permeability coefficients ($Pe_{in\ vivo}$) by dividing PS by an estimated value of the surface area of perfused capillaries equal to 100 cm^2/g and the log natural of the BBB permeability coefficients were normalized for molecular weight. On analyzing the slope of eq. **4**, the authors concluded that the *in vitro* BBB model overestimated the $Pe_{(in\ vivo)}$ values by approximately 150-fold; and in the case of compounds crossing the BBB by carrier mediated influx such as L-DOPA or D-glucose, the overestimation was also of several orders of magnitude. This fact was attributed to the downregulation in tissue culture of the BBB nutrient transporters.

$$\ln (Pe_{(in\ vitro)} \times \sqrt{Mw}\ ) \quad (5)$$

$r^2 = 0.859$ r = 0.927 s = 0.719 n = 13 F = 66.77

$$\ln (Pe_{(in\ vivo)} \times \sqrt{Mw}\ ) = 9.96 + 2.146 \ln (Pe_{(in\ vitro)} \times \sqrt{Mw}\ ) \quad (6)$$

(0.000) (0.000)

$r^2 = 0.897$ r = 0.947 s = 0.978 n = 13 F = 95.53

In these equations and in all the ones below, n is the number of compounds, s is the standard deviation, r^2 is the squared correlation coefficient, r is the correlation coefficient, F is the Fisher F-statistic, and the figures in parentheses are the P-values of coefficients. On analyzing eqs. **4** and **5**, there appears to be a disagreement with the results obtained by Garberg *et al.* [47]; however, this may be explained by the choice of the compounds studied. Dehouck *et al.* [49], studied 13 compounds, 10 of which are transported by passive diffusion; while Garberg *et al.* [47] investigated 22 compounds and only 10 are transported across the BBB by passive diffusion. Moreover, another interesting point to highlight is the fact that the slopes of eqs. **4** and **6** are essentially identical, which provides additional support to the above-mentioned analysis.

Table 2. Correlation Matrix of Permeability Data for Compounds Studied by Garberg *et al.* [47]

	logPapp(cm/s)[a]	logPe(cm/s)[b]	logPe(cm/s)[c]	logPe(cm/s)[d]	logPapp(cm/s)[f]	logPapp(cm/s)[g]	logPapp(cm/s)[h]
logPe(cm/s)[b]	**0.660**						
logPe(cm/s)[c]	**0.337**	0.333					
logPe(cm/s)[d]	**0.462**	0.500	0.615				
logPapp(cm/s)[f]	**0.631**	0.891	0.265	0.362			
logPapp(cm/s)[g]	**0.689**	0.865	0.282	0.429	0.973		
logPapp(cm/s)[h]	**0.630**	0.867	0.388	0.613	0.931	0.941	
logPapp(cm/s)[i]	**0.635**	0.806	0.391	0.520	0.853	0.866	0.867

(a) The apparent permeability coefficients obtained *in vivo* by mouse brain uptake assay (MBUA). (b) The endothelial permeability coefficients from BBEC co-cultured with rat astrocytes, obtained from transport in the apical to basolateral direction (a>b). (c) The endothelial permeability coefficients from human primary brain endothelial cells (HPBEC) for (a>b) transport. (d) The endothelial permeability coefficients from SV40 immortalized rat brain endothelial cells (SV-ARBEC) for (a>b) transport. (f) The apparent permeability coefficients from Madin-Darby canine kidney ($MDCK_{ATCC}$) cells for (a>b) transport. (g) The apparent permeability coefficients from Madin-Darby canine kidney ($MDCK_{WT}$) cells for (a>b) transport. (h) The apparent permeability coefficients from Madin-Darby canine kidney ($MDCK_{mdr\text{-}1}$) cells for (a>b) transport. (i) The apparent permeability coefficients from Caco-2 cells for (a>b) transport.

Another important study has been recently conducted by Dehouck *et al.* [49], with the objective of evaluating whether the *in vitro* model currently used by AstraZeneca (Södertälje, Sweden), employing BBMEC co-cultured with primary rat astrocytes, is able to give accurate predictions of *in vivo* BBB permeability. In addition, a comparative study was performed to evaluate the equivalence between both, BBMEC and Caco-2 *in vitro* models, for predicting the *in vivo* BBB transport. The studied compounds along with permeability values obtained from *in vivo* (BUI and PS) and *in vitro* models (BBMEC and Caco-2) are shown in Table **3**. Interestingly, good correlations were found by the authors between the BUI or PS values available for 13 out of the 20 compounds studied and the corresponding permeability coefficients measured on BBMEC cultures. In contrast, poor correlations were obtained between Caco-2 cell data and *in vivo* BBB data. The best regression equations found by the authors were as follows:

$$\ln (BUI \times \sqrt{Mw}\ ) = 14.0 + 1.278$$

(0.000) (0.000)

There are several other studies, which have compared *in vitro* BBB permeability and CNS uptake [51-56, 64]. However, due to inherent difficulties in the experimental determination of *in vivo* BBB data, only smaller sets of data have been used to derive *in vivo* / *in vitro* correlations. Finally, it should be noted that special expectations have been directed towards a new *in vitro* BBB model developed recently by Terasaki *et al.* [46]. They have demonstrated that brain endothelial cell lines derived from transgenic animals (TM-BBB and TR-BBB from mouse and rat, respectively) retain better the *in vivo* functions compared with traditionally immortalized cell lines. Furthermore, the *in vivo* and *in vitro* comparison showed that these immortalized BBB cell lines express most of transporters that are expressed *in vivo*. Thus, the TR-BBB and TM-BBB cells

Table 3. ***In vivo*** **and** ***in vitro*** **Permeability Data for Compounds Studied by Dehouck** ***et al.*** **[49]**

Compound	Transport[e]	M_W	Pe x 10^{-6} (cm/s)[a]	BUI (%)[b]	PS (ml/g/mim)[c]	Papp x 10^{-6} (cm/s)[d]
Acetylsalicylic acid	Diffusion	180	9.0	1.8	nr	9.09
Antipyrin	Diffusion	188	179.2	68	1.0	nr
Caffeine	Diffusion	194	229.7	90	1.2	30.8
Codeine	Diffusion	299	171.7	26	0.2	nr
Dexamethasone	Eflux	392	19.2	nr	nr	12.2
Diazepam	Diffusion	285	227.7	nr	1.2	33.4
Dopamine	Diffusion	153	22.5	3.9	nr	9.33
Hydrocortisone	Eflux	362	29.7	1.4	0.0084	14.0
Lidocaine	Diffusion	234	293.3	nr	0.76	nr
Mannitol	Diffusion	182	13.0	1.9	0.00125	0.38
Morphine	Efflux	285	33.3	2.6	0.03	nr
Nicotine	Diffusion	162	289.3	131	nr	19.4
Phenytion	Diffusion	252	106.7	31	0.3	26.7
Pindolol	Diffusion	248	44.0	nr	nr	16.7
Pirenzepine	Diffusion	351	11.8	nr	nr	0.44
Propranolol	Diffusion	259	294.3	75	0.67	21.8
Sucrose	Diffusion	342	8.3	1.4	0.0003	1.71
Terbutaline	Diffusion	225	10.7	nr	nr	0.47
Urea	Diffusion	60	63.5	2.4	0.004	4.56
Vincristine	Efflux	825	8.0	nr	0.006	nr

(a) The endothelial permeability coefficients from BBEC co-cultured with rat astrocytes. (b) The relative permeabilities obtained *in vivo* in rat by brain uptake index (BUA). (c) The permeability-surface area products obtained from brain perfusion technique. (d) The apparent permeability coefficients from Caco-2 cells. (e) Classifications were made made according to Seelig [50]. Note: nr = not reported in the original publication.

appear to be a useful and promising *in vitro* BBB model for the study of drug transport across the BBB.

4. QSAR MODELS TO PREDICT BBB PERMEATION

This review focuses on both physicochemical and theoretical QSAR methods for the prediction of drug transport across the blood-brain barrier (BBB), and special emphasis will be given to recent progress that has been made in the modeling of BBB permeability data. For the purposes of this review, the reported QSAR models will be divided into three classes: those based on BBB permeability data (e.g. log PS), those based on measures of brain-blood distribution at the steady state (log BB), and the classification approaches based on qualitative brain penetration data.

4.1 QSAR Models Based On BBB Permeability Data

Lipophilicity and molecular size have long been recognized as key factors regulating the entry of compounds into the CNS. In the late 1950s, Mayer *et al.* [58] were among the first to use partition coefficients (heptane-buffer) to model the entry of drugs into the brain. Some years later, Hansch *et al.* [59] were the first ones to use the partition coefficient between n-octanol and water (log Poct) as a general predictor of BBB permeability. They found a parabolic relationship between the π substituent constant and the concentration of thirteen benzeneboronic acid analogues measured in mouse brain. The regression equation, which has recently been placed by the authors in bilinear form and using calculated log Poct values (CLOGP) [60], was as follows:

$$\log BC = 1.91 (\pm 0.35) CLOGP - 2.14 (\pm 0.51) \log (\beta 10^{CLOGP} + 1) - 0.04 (\pm 0.22) \quad (7)$$

$r^2 = 0.972$ r = 0.986 s = 0.073 n = 13, log P_O = 1.87 (± 0.56)

In this expression, BC is the brain concentration measured 15 min after injection of a dose of boron, and the values in parentheses are the 95% confidence intervals of the regression coefficients. This equation shows that an increase

of log Poct value by over 1.87 will result in a lower brain penetration of the compounds. From this and similar studies as well as from several correlations between drug potency and log Poct values, Hansch *et al.* have suggested that there exists a non-linear relationship between brain uptake and lipophilicity, with an optimum log Poct value of about 2 [61].

In a recent review, the influence of lipophilicity on the BBB permeability was reevaluated by Bodor and Buchwald [71]. The authors collected *in vivo* permeability data from the literature for more than 70 compounds representing a wide range of permeability and lipophilicity. The log Poct parameter was used as independent variable; for some compounds however, the log $D_{7.4}$ was used instead of log Poct. After omitting several outlier compounds, the following equation was derived for 58 structurally diverse compounds:

$$\log Pc_{(cm/s)} = -5.102 + 0.566 \log Poct \quad (8)$$
$$(\pm 0.081) \quad (\pm 0.038)$$

$r^2 = 0.803$ r = 0.896 s = 0.617 n = 58 F = 226.8

where log $Pc_{(cm/s)}$ is the logarithm of capillary permeability coefficient measured in rat brain (for some compounds, the Pc values were from guinea pig). The obtained equation represents a very reasonable correlation but, due to the fact that no numerical details were given in the original publication, it is not possible to evaluate the contribution of other factors to BBB permeability.

Another important physicochemical property affecting drug transfer across the BBB is the molecular size. The permeation (P_m) of a drug through biological membranes depends not only on the membrane partition coefficient (K_m) but also on the drug's diffusion coefficient, according to the following equation: $P_m = (D_m \times K_m) / L$, where D_m is the membrane diffusion coefficient of the drug and L is the membrane thickness. Thus, although P_m is mainly influenced by K_m (frequently modeled by log Poct), the passive diffusion of drugs across biological membranes depends also on D_m. Furthermore, according to Sutherland and Einstein's relation, the diffusion coefficient of a solute is inversely related to their molecular weight ($D_m \propto [Mw]^{1/3}$) [74].

The first quantitative evaluation of the influence of molecular size on BBB permeability was made by Levin [62], who derived the following equation for 22 out of a total of 27 miscellaneous drugs:

$$\log Pc_{(in\ vivo)} = -4.605 + 0.412 \log (Poct / \sqrt{Mw}) \quad (9)$$
$$(0.000) \ (0.000)$$

$r^2 = 0.826$ r = 0.910 s = 0.432 n = 22 F = 94.70

where log $Pc_{(in\ vivo)}$ is the logarithm of capillary permeability coefficient measured *in vivo* by using the single time point method. The 27 structurally diverse compounds studied by Levin covered a wide range of molecular size (18 to 1400 Da) and lipophilicity (-4.04 to 3.19). The excluded compounds were water and the four compounds with molecular weights greater than 500 Da (bleomycin, adriamycin, vincristine, and epipodophyllotoxin). Levin's model supports the hypothesis of molecular weight threshold for the drug transport across the BBB; that is, lipophilic drugs with molecular masses above 500 Da will be physically impeded to cross the BBB in pharmacologically significant amounts. Reanalyzing Levin's data, Hansch *et al.* [61] derived a similar relationship but using the log Poct and log *Mw* as independent variables. The reported correlation equation, which was checked from the original paper, was as follows:

$$\log Pc_{(in\ vivo)} = -1.939 + 0.494 \log Poct - 1.373 \log Mw$$
$$(0.002) \ (0.000) \quad (0.000) \quad (10)$$

$r^2 = 0.895$ r = 0.946 s = 0.398 n = 23 F = 85.17

In this case, only four compounds were excluded: ascorbate, adriamycin, vincristine, and epipodophyllotoxin. This equation is slightly better that eq. **9** and included one more data point. Furthermore, the exclusion of ascorbate may be justified because it has been reported that dehydroascorbic acid (the oxidized form of ascorbic acid) is transported into the brain *via* the hexose transporter, GLUT1 [69]. There are several other studies which have demonstrated the importance of molecular size in the drug transport across the BBB (see ref [61]). For example, Cornford *et al.* [70] derived a reasonable correlation between the brain uptake index (BUI) and the log Poct for a series of 48 structurally diverse compounds. The BUI indexes were normalized to the compound's molecular weight and the obtained correlation is shown in Fig. (**2**). Following a similar line of analysis, Lien [8] related the BUI values of twenty radiolabeled drugs reported by Oldenford (see ref [8]) to lipophilicity, which was expressed as the logarithm of olive-oil/water partition coefficient, and molecular weight. The obtained regression equation was as follows:

$$\log BUI = 0.346 \log P_{(olive\ oil/w)} - 0.814 \log Mw + 3.587 \quad (11)$$

$r^2 = 0.712$ r = 0.844 s = 0.436 n = 20

Equations of Cornford and Lien clearly show the dependence of BUI on the molecular size and suggest that under isolipophilic condition, a compound with lower molecular weight will have higher brain uptake.

As an attempt to consolidate all the observations of the effect of molecular size on BBB permeability, Kaliszan and Markuszewski [68] proposed a general model for the description of BBB permeability, which is expressed by the following equation: log BB = k_1 log Poct – k_2 DIS + k_3, were k_1-k_3 are general constants obtained from the model and DIS is a molecular bulkiness descriptor (e.g. Mw). The model proposed was shown to apply to four brain/blood data set, two of which corresponded to kinetic measures of brain uptake. The reported correlation equations were as follows:

$$\log Pc_{(in\ vivo)} = -4.288 + 0.431 \log Poct - 0.0035 \ Mw$$
$$(0.000) \ (0.000) \quad (0.000) \quad (12)$$

$r^2 = 0.881$ r = 0.939 s = 0.359 n = 22 F = 70.45

$$\log BUI = -1.844 + 0.417 \log Poct - 0.0027 \ Mw \quad (13)$$
$$(0.000) \ (0.000) \quad (0.058)$$

$r^2 = 0.621$ r = 0.788 s = 0.458 n = 18 F = 12.26

Equation **12** was based on Levin's data set and the compounds excluded were water, creatinine, adriamycin, epipodophyllotoxin and bleomycin (note that vincristine was

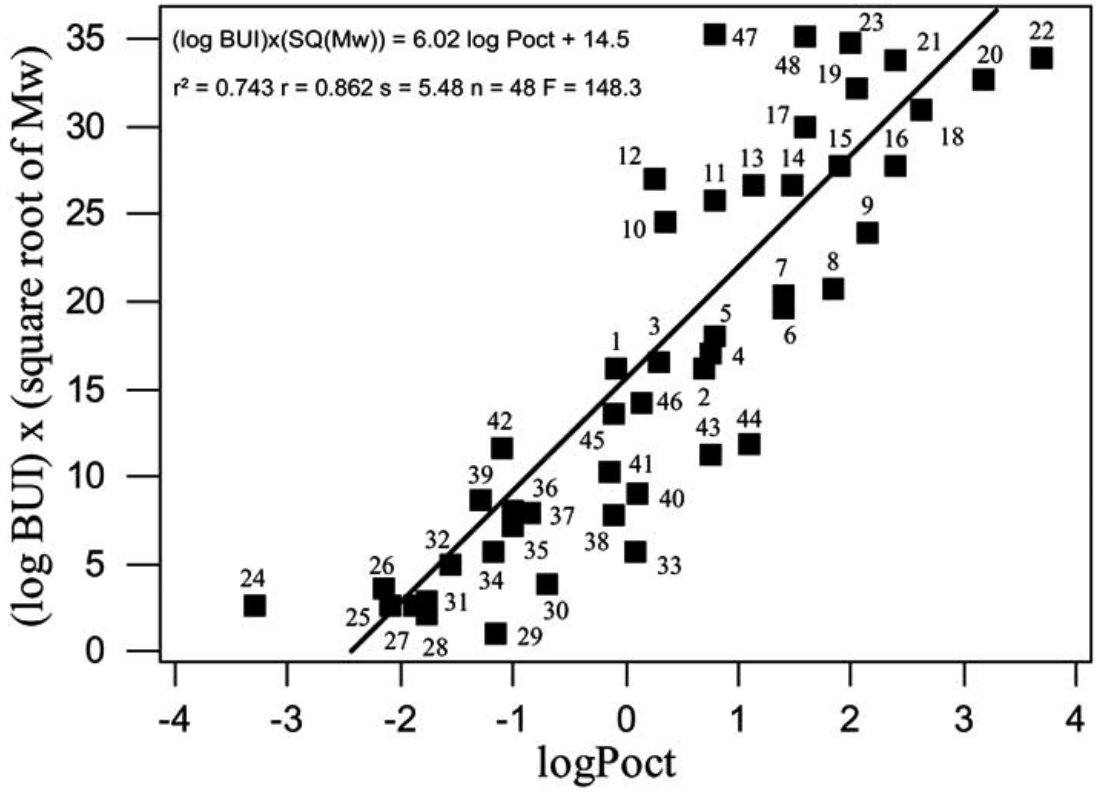

Fig. (2). Correlation reported by Cornford *et al.* [70] between the brain uptake index normalized by the molecular weight (log BUI x $\sqrt{Mw}$) and log octanol/water partition coefficient (log Poct) for 48 compounds. Compounds key: **1**:isopropanol, **2**:n-butyric acid **3**: n-propanol, **4**: 3,4-dimethoxy PEA, **5**: n-butanol, **6**:phenobarbital, **7**:B-PEA, **8**:hexanoate **9**:octanoate, **10**:antipyrine, **11**:codeine, **12**:caffeine, **13**:nicotine, **14**:tryptophol, **15**: pen-tobarbital, **16**:dilantin, **17**:corticosterone, **18**:estradiol, **19**:lidocaine, **20**:testosterona, **21**: imipramine, **22**:progesterone, **23**:cocaine, **24**:sucrose, **25**:mannitol, **26**:urea, **27**:glucose, **28**:glycerol, **29**:hypoxanthine, **30**:thymine, **31**:fructose, **32**:epinephrine, **33**:5-hydroxy tryptamine, **34**:acetylsalicylic acid, **35**:dopamine, **36**:thiourea, **37**:ascorbate, **38**:acetyl choline, **39**:norepinephrine, **40**:morphine, **41**:adenine, **42**:uracil, **43**:mescaline, **44**: aldosterone, **45**:tryptamine, **46**:ethanol, **47**:diacetyl morphine, **48**: amphetamine sulfate.

included). On the other hand, equation **13** was based on the brain uptake indexes (BUI) reported by Cornford *et al.* [70], measured in newborn rabbit for 18 structurally diverse compounds representing a wide range in molecular size and lipophilicity (Mw from 32 to 369 Da, and logPoct from -2.11 to 3.28). In order to evaluate the contribution of molecular size to BBB permeability, we have reanalyzed Levin's data using the same compounds included by Levin in eq. 8. The obtained equation was as follows:

$$\log Pc_{(in\ vivo)} = -4.791 + 0.423 \log Poct - 0.054\ (Mw/100)^2 \quad (14)$$

(0.000) (0.000) (0.027)

$r^2 = 0.859$ r = 0.927 s = 0.398 n = 22 F = 58.04

From a statistical point of view, the quality of this equation is good and similar to equations **9** and **12** reported, and the logPoct and $(Mw)^2$ descriptors are not intercorrelated (r^2 =0.053, n=22). However, the point that we want to highlight is that there is a significant non-linear relationship between log Pc and Mw despite the omission of all compounds of Mw >500. In Fig. (**3**) an empirical lorentzian function was drawn, which clearly shows the existence of an optimal molecular weight range for BBB permeation (200-300 Da). It should be noted that the rather large degree of observed scatter is due to the fact that transcellular permeation depends on both molecular size and lipophilicity, as shown by eqs. **9**-**14**. According to Pardridge [57], the molecular threshold hypothesis may be explained within the context of pore model ("molecular hitchhiking") of lipid-mediated transport across biological membranes proposed by Träuble [66]. An important additional support to this hypothesis comes from the work of Seelig *et al.* [67], who used the air-water partition coefficient (K_{aw}), the critical micelle concentration and the cross-sectional area (A_D) to distinguish between compounds with ability to cross or not cross the BBB by passive diffusion. Three groups of compounds were identified: very hydrophobic compounds with large K_{aw} coefficients and with $A_D > 80$ Å^2 ($Mw \cong$350-450 Da) which do not cross the BBB in significant amounts, compounds with lower K_{aw} coefficients and an average $A_D \cong 50$ Å^2 (Mw about 250 Da) which easily cross the BBB, and finally hydrophilic compounds with $A_D < 50$ Å^2 which cross the BBB only if applied at high concentrations. The consistency of these experimental results provides further confidence than the obtained results from eq. **14** (see Fig. **3**) are not artifactual, and besides they evidence the exceptional quality of the QSAR study made by Levin [62].

In contrast to the molecular weight threshold model, an alternative model has been proposed to explain the reduced BBB transport of compounds with a molecular mass of >

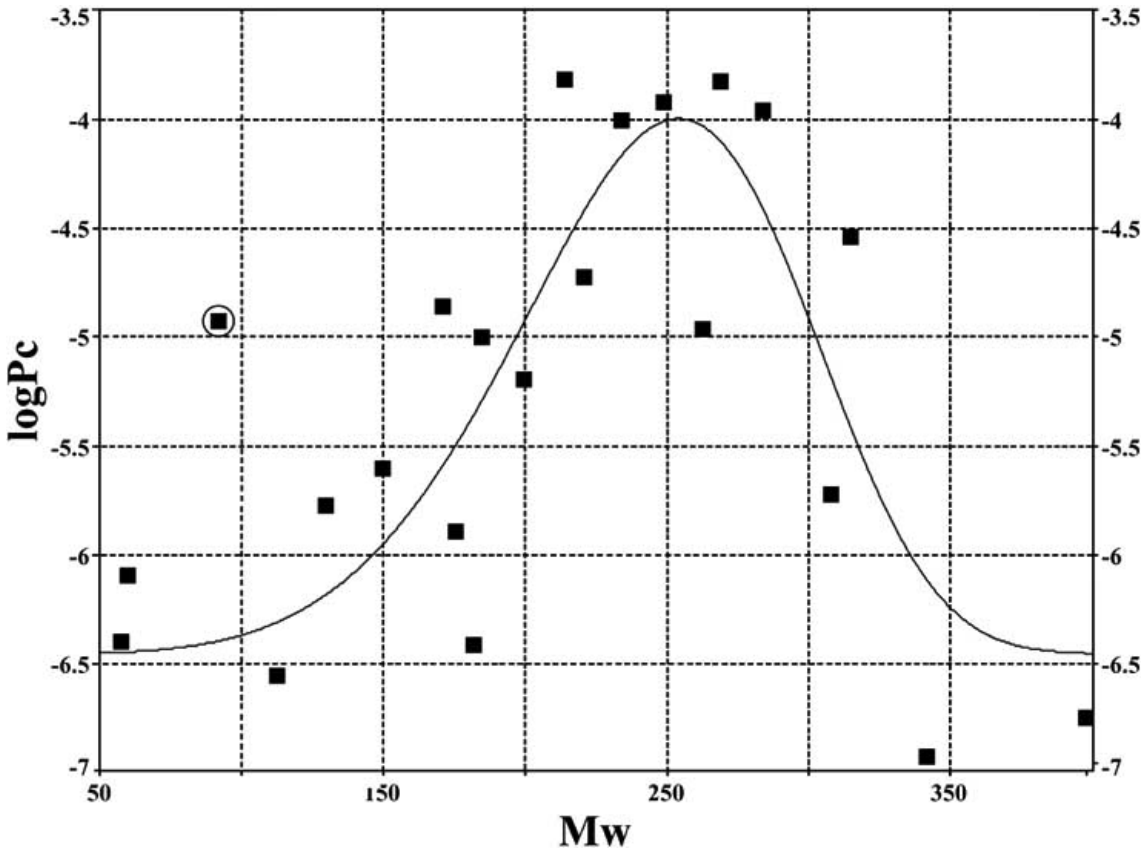

Fig (3). Relationship between logarithm of capillary permeability coefficient measured *in vivo* (log $Pc_{(in\ vivo)}$) and molecular weight (*Mw*) for Levin's data set (water, bleomycin, adriamycin, vincristine, and epipodophyllotoxin were omitted). To note that labeled point (circle) corresponds to creatinine.

400-600 Da. This hypothesis is based on the existence of multiple efflux systems at the brain capillary endothelium such as the P-glycoprotein (P-gp) and the multidrug-resistance proteins (MRPs) [28]. On this basis, lipophilic and large molecules (Mw> 400-600 Da) should hardly penetrate the BBB in general. For example, of the five compounds omitted from eqs. **9** and **14**, three (adriamycin, vincristine, and epipodophyllotoxin) are substrates for either P-gp or MRPs or both [50], whereas bleomycin is apparently not affected by P-gp activity [63] due to its strong hydrophilic nature (log Poc = -3.3). There are, however, several examples of drugs with a molecular mass below the threshold of 400-600 Da which are unable to gain access to the brain, some of them are AZT (log $Poct_{(exp)}$ = 0.05, Mw = 267), p-aminohippuric acid (log $Poct_{(exp)}$ = -0.89, Mw = 194), benzylpenicillin (log $Poct_{(exp7.4)}$ = -1.81, Mw= 334), valproic acid (log $Poct_{(exp7.4)}$ = 0.13, Mw= 144), homovanillic acid (log $Poct_{(exp)}$ = 0.33, Mw = 182), 5-hydroxyindolacetic acid (log $Poct_{(CLOGP)}$ = 0.74, Mw= 191), and others. However, recently it has become clear that many of these compounds are substrates of several other transporters that exclude drugs from the brain, such as the organic anion transport proteins (Oatps) and the organic anion transporters (OATs) [24]. Thus, the presence of these transporter systems at the brain capillary endothelial cells provides a novel explanation for the brain to blood efflux transport of these drugs. Although the influence of the influx and/or efflux systems on QSAR modeling will be discussed later, an important aspect to highlight now is that eqs. **9** and **14** were derived by omitting the P-gp substrates and bleomycin (all with Mw >500 Da). The term [log (Poct / $\sqrt{Mw}$)] of eq. 9, however, is significant at the level of at least 0.0001 and *Mw* (eq. **14**) at the level of 0.027.

There are other studies which have examined the influence of both lipophilicity and molecular size on BBB permeability but using data obtained from *in vitro* cell culture systems. For example, Shah *et al.* [76] studied the permeabilities of 14 solutes of varying lipophilicity (-2.97 to 3.54) employing BBMECs cultured on collagen-coated polycarbonate membranes. An excellent correlation was established between the permeability coefficients (P_m) of the solutes and the function log [Poct/$(Mw)^{1/2}$]:

$$P_{m\ (in\ vitro)} = 58.69 + 15.11 \log (Poct / \sqrt{Mw}\ ) \qquad (15)$$
$$(0.000)\ (0.000)$$

$r^2 = 0.967$ r = 0.983 s = 6.88 n = 14 F = 349.5

It should be noted that a significant correlation was also obtained when both log Poct and log Mw were used as independent variables instead of the molecular weight function ($r^2 = 0.908$) [61].

More recently Chikhale *et al.* [77] used the rat brain perfusion technique to obtain permeability coefficients for seven model peptides (see structures in Fig. **5**). They found a poor correlation between the permeability coefficients ($P_{in\ situ}$) and the corresponding log Poct values, whereas a much better correlation was found when the n-heptane-ethylene

glycol partition coefficient (log $P_{(hep\text{-}gly)}$) was used instead of log Poct:

$$\text{Log } P_{(in\ situ)} = -3.696 + 0.464 \log P_{(hep\text{-}gly)} \quad (16)$$
$$(0.000)\ \ (0.002)$$

$r^2 = 0.883$ r = 0.939 s = 0.271 n = 7 F = 37.64

Interestingly, it was also shown by the authors that the BBB permeability of studied peptides strongly depends on the hydrogen-bond capacity of the amide nitrogens, since good correlations were obtained for log $Pc_{(in\ vivo)}$ against the number of potential hydrogen bonds (H-bond) and against the Seiler's ΔlogP parameter, which is an experimental measure mainly of the solute hydrogen-bond acidity [78] (r = 0.962 for ΔlogP, and r = 0.906 for H-bond).

As made earlier for Levin's data, we have reanalyzed this data set and derived the following equation:

$$\log Pc_{(in\ vivo)} = 0.160 + 0.503 \log P_{(hep\text{-}gly)} - 1.382 \log Mw$$
$$(0.902)\ \ (0.000)\qquad (0.032)\qquad (17)$$

$r^2 = 0.968$ r = 0.984 s = 0.159 n = 7 F = 59.88

To note that log $P_{(hep\text{-}gly)}$ and log Mw descriptors are not intercorrelated (r^2 =0.07). Even though this equation was based on too small a number of data points, the log Mw term is significant statistically and clearly it shows that the size-restriction imposed by the BBB can appropriately be modeled by the log Mw term.

Following a different line of analysis, Gratton *et al.* [79] used the general solvation equation of Abraham *et al.* [80, 81] to estimate the BBB permeation of 18 structurally diverse compounds. They related the BBB PS products to Abraham's solvation parameters such as the solute dipolarity/polarizability (π_2^H), the solute overall or effective hydrogen-bond basicity and acidity ($\sum\beta_2^H$, $\sum\alpha_2^H$), the excess molar refraction (R_2) and the characteristic volume of McGowan (Vx). The PS products were determined by means of the *in situ* perfusion technique using protein-free saline at pH 7.4 as perfusate. The reported equation was as follows:

$$\log PS = -1.213 + 0.77\, R_2 - 1.87\, \pi_2^H - 2.80 \sum\beta_2^H + 3.31\, Vx$$
$$(0.000)\ (0.033)\ \ (0.000)\ \ \ (0.000)\ \ \ \ (0.000) \quad (18)$$

$r^2 = 0.953$ r = 0.976 s = 0.481 n = 18 F = 65.28

The $\sum\alpha_2^H$ term was not significant and was omitted from eq. **18** by the authors. The statistical quality of this equation is quite good and clearly shows the positive dependence of log PS on the molecular size as reflected by Vx and R_2, as well as the large negative influence that the molecular polarity (π_2^H and $\sum\beta_2^H$) has on the BBB permeability. An important aspect to highlight of this study is that the brain uptake of the analyzed compounds was demonstrated to be by passive diffusion. Therefore, taken into account the wide range of molecular weight and log Poct of the studied compounds (see Table **4**), we reanalyzed this data set and derived the following equation:

$$\log PS = -1.749 + 0.889 \log Poct - 0.087\, (Mw/100)^2 \quad (19)$$
$$(0.000)\ \ (0.000)\qquad (0.000)$$

$r^2 = 0.924$ r = 0.961 s = 0.568 n = 18 F = 90.71

Table 4. Molecular descriptors and Observed and Calculated log PS values From Eq. 24 for Compounds Studied by Abraham [82]

Compound	logPS Observed(a)	logPS Calculated(b)	logPoct	Vx	R2	Pi	Alfa	Beta	Mw
Erythritol (d)	-4.57	-3.65	-2.29	0.9070	0.620	1.20	0.70	1.40	122.12
Urea (d)	-3.79	-4.55	-2.11	0.4648	0.500	1.00	0.50	0.90	60.06
Ethylene glycol (d)	-2.99	-3.55	-1.36	0.5078	0.404	0.90	0.58	0.78	62.07
Thiourea (d)	-3.36	-2.28	-1.02	0.5696	0.640	0.70	0.78	0.86	76.12
2-Propanol (d)	-1.66	-0.71	0.05	0.5900	0.212	0.36	0.33	0.56	60.10
Ethanol (d)	-1.52	-1.53	-0.30	0.4491	0.246	0.42	0.37	0.48	46.07
Antipyrine (d)	-2.00	-1.87	0.20	1.5502	1.320	1.50	0.00	1.48	188.23
Mannitol (d)	-5.01	-4.73	-3.20	1.3062	0.836	1.80	0.70	1.92	182.17
Sucrose (d)	-5.30	-5.62	-3.70	2.2279	1.970	2.50	2.10	3.20	342.29
Oestradiol (d)	-0.83	-1.49	2.69	2.1988	1.800	3.30	0.88	0.95	272.39
Thymine (d)	-1.93	-2.05	-0.62	0.8925	0.800	1.00	0.44	1.03	126.11
22001 (d)	-0.82	-0.66	1.55	1.4120	1.710	1.30	0.40	1.10	216.21
12002 (d)	0.71	-0.05	3.80	2.2620	2.561	2.11	0.60	1.20	391.19
11003 (d)	-0.75	-1.37	3.63	3.9830	2.121	3.78	0.73	2.57	503.03
95005 (d)	-1.95	-1.90	1.26	2.0770	1.354	2.46	0.77	1.50	251.32
26006 (d)	-1.79	-2.18	3.90	4.7800	3.353	5.29	2.08	3.11	6.22.67

(Table 4)contd.....

Compound	logPS Observed(a)	logPS Calculated(b)	logPoct	Vx	R2	Pi	Alfa	Beta	Mw
13007 (d)	1.13	0.73	2.19	1.1510	0.673	0.55	0.16	0.61	163.26
Propranolol (d)	0.98	0.64	3.65	2.1480	1.843	1.50	0.60	1.27	259.35
CP20	-1.89	-2.56	-0.77	1.0745	0.977	1.31	0.10	1.21	139.00
CP21	-1.48	-2.14	-0.31	1.2154	0.932	1.31	0.10	1.21	153.00
CP24	-0.64	-1.30	0.70	1.4972	0.918	1.31	0.10	1.21	181.00
CP29	-0.38	-0.89	1.24	1.6381	0.915	1.31	0.10	1.21	195.00
CP25	-0.36	-0.41	1.90	1.7790	0.905	1.31	0.10	1.21	209.00
CP94	-1.03	-1.68	0.23	1.3563	0.894	1.31	0.10	1.21	167.00
AcFNH2(I)	-3.80	-4.42	0.05	1.6519	1.453	3.90	0.65	0.89	206.00
AcFFNH2(II)	-4.28	-3.68	1.19	2.7979	2.466	5.20	0.67	1.63	353.00
AcFFFNH2(III)	-4.39	-3.53	2.30	3.9439	3.479	6.60	0.64	2.27	500.00
AcFF(NMeF)NH2(IV)	-3.74	-3.24	2.63	4.0848	3.441	6.45	0.50	2.37	514.00
AcF(NmeF)2NH2(V)	-3.31	-3.40	2.53	4.2257	3.403	6.60	0.16	2.48	528.00
Ac(NmeF)3NH2(VI)	-2.47	3.10	2.92	4.3666	3.365	6.50	0.00	2.50	542.00
Ac(NmeF)3NHMe(VII)	-2.06	-2.74	3.24	4.5075	3.302	6.10	0.00	2.55	556.00
Corticosterone	-2.29	-2.07	1.94	2.7389	1.860	3.43	0.40	1.63	346.46
Aldosterone	-3.46	-2.73	1.08	2.6890	2.010	3.47	0.40	1.90	360.45
Hydrocortisone	-3.85	-2.40	1.55	2.7976	2.030	3.49	0.71	1.90	362.46
Estradiol(c)	-1.74		4.01	2.1988	1.800	1.77	0.86	1.10	272.39
Testosterone	-1.72	-0.48	3.31	2.3827	1.540	2.59	0.32	1.19	288.43
Progesterone	-1.74	-0.68	3.70	2.6215	1.450	3.29	0.00	1.14	314.47
Glycerol	-2.98	-3.05	-1.76	0.7074	0.512	0.90	0.70	1.14	92.09

(a) Observed log PS Values in cm3 s-1 g-1. (b) Calculated log PS Values from Eq **24**. (c) Compound not Usedto Derive Eq.**24**. (d) Log PS Values and Molecular Descriptors Values taken from [79]

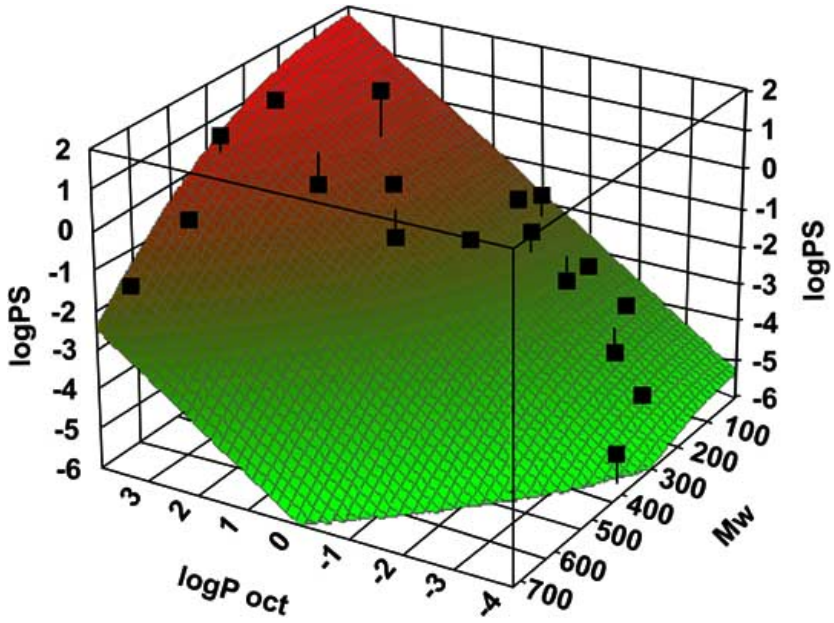

Fig (4). Three dimensional plot of log PS versus the log Poct and Mw parameters as well as the corresponding response surface obtained from Eq. **19**.

This equation is highly significant statistically and the $(Mw)^2$ and log Poct terms are weakly intercorrelated (r^2 = 0.325). Significant correlations, though with slightly worse performance, were obtained when Mw or log Mw were used to derive eq. **19** instead of $(Mw)^2$ term (r^2 range 0.91 and 0.85, respectively). Equation **19** again emphasizes that there is an optimum size for the entry of compounds into the CNS. Fig. (**4**) shows the three dimensional plot of log PS versus the log Poct and Mw parameters as well as the corresponding response surface obtained from eq. **19**.

Very recently, Abraham [82] constructed a new data set of 38 compounds in order to derive a more general model. The PS values used were mainly based on those determined by Gratton *et al.* [79] and the ones reported by Habgood *et al.* [83], Chikhale *et al.* [77], and Pardridge and Mietus [84]. Table **4** lists the PS values for the 38 compounds along with the values of molecular weight and octanol-water partition coefficient, and Fig. (**5**) shows the chemical structures for some of these compounds. After excluding compounds 22001, 12002, 11003, 95005, 26006, 13007, propranolol (all partially ionized at pH 7.4) and sucrose, the following equation was reported:

$$\log PS = -0.716 - 0.974\,\pi_2^H - 1.802\,\Sigma\alpha_2^H - 1.603\,\Sigma\beta_2^H + 1.893\,Vx \quad (20)$$

(0.073) (0.000) (0.000) (0.001) (0.000)

$r^2 = 0.868$ r = 0.932 s = 0.52 n = 30 F = 41.18

In this case, the R_2 term was not significant and was omitted from eq. **20**. The statistical quality of this equation is quite reasonable as indicated by the s, r and F-test parameters. Qualitatively, equations **18** and **20** are similar in that increasing solute size enhances BBB permeability whereas increasing polarity has the opposite effect.

Reanalyzing this new Abraham's data set, we obtained again a very reasonable two-parameter equation based on log Poct and Mw:

$$\log PS = -0.224 + 1.301 \log Poct - 1.187\,(Mw/100) \quad (21)$$

(0.443) (0.000) (0.000)

$r^2 = 0.791$ r = 0.889 s = 0.745 n = 30 F = 51.06

This equation was derived by using the following compounds: sixteen Gratton's compounds, excluding sucrose (also omitted by Abraham) and mannitol, which is not an outlier but has a large influence on the regression equation, six Habgood's compounds, and glycerol as well as seven Chikhale' peptides (see Table **4**). The compounds removed to obtain eq. **21** were the six steroids (corticosterone, aldosterone, hydrocortisone, estradiol, testosterone and progesterone) studied by Pardridge and Mietus [84]. It should be noted, however, that the exclusion of these compounds was justified since, as demonstrated by Barnes *et al.* [85], most steroids are efficiently transported by P-glycoprotein in *in vitro* models of multidrug-resistant cells. Moreover, *in vivo* studies have also indicated that some steroid compounds such as aldosterone, hydrocortisone, corticosterone and dexamethasone are effluxed from the brain *via* P-gp [24, 50].

Another important aspect to consider in relation to eqs **19** and **21** is the high collinearity that exists between Mw and most of solvation parameters. The r^2 values corresponding to the data set used in eq. **21** were: Mw/R_2 0.93, Mw/π_2^H 0.83, Mw/$\Sigma\beta_2^H$ 0.85, and Mw/$\Sigma\alpha_2^H$ 0.06. Due to this fact, it could be argued that Mw is conveying information about the molecular polarity in these equations and, therefore, the effect of molecular size would be confounded with that of polarity as expressed by the π_2^H and $\Sigma\beta_2^H$ parameters. In order to break down the multicollinearity and to be able to treat the effects of both polarity and molecular mass separately, a sub set was constructed by omitting all compounds with a molecular mass of > 500 Da (peptides III, IV, V, VI, VII and compounds 11003 and 26006). The r^2 values between pairs of descriptors for this sub set of 23 compounds were as follows: Mw/log Poct 0.62, Mw/π_2^H 0.52, Mw/ $\Sigma\beta_2^H$ 0.35, and Mw/$\Sigma\alpha_2^H$ 0.025. Again, a quite reasonable equation was obtained:

$$\log PS = -0.077 + 1.294 \log Poct - 1.274\,(Mw/100) \quad (22)$$

(0.871) (0.000) (0.000)

$r^2 = 0.808$ r = 0.899 s = 0.744 n = 23 F = 42.10

Equation **22** clearly shows that the negative influence of molecular size on log PS is not an artifact arising from the multicollinearity between Mw and π_2^H and/or $\Sigma\beta_2^H$ parameters. Finally, the best regression equation that we found for all compounds (except estradiol) described in Table **4** was as follows:

$$\log PS = -1.054 + 0.796 \log Poct - 0.724\,\pi_2^H \quad (23)$$

(0.000) (0.000) (0.000)

$r^2 = 0.844$ r = 0.918 s = 0.663 n = 37 F = 92.14

This equation is highly significant statistically and the π_2^H and log Poct terms are weakly intercorrelated (r^2 = 0.283). It should be noted, however, that the π_2^H descriptor is not based entirely on solute dipolarity but also on molecular polarizability, which is a property closely related to molecular size. In an attempt to treat the information encoded by π_2^H separately, it was normalized to the compound's size by dividing its value by (Mw/100). The resulting descriptor, π_2^{NOR}, is physically justified since the influence of molecular dipole moment on solvation phenomena will vary with the solute molecular size. As expected, an identical correlation to eq. **23** was obtained when π_2^{NOR} and (Mw/100) were used to derive eq. **24** instead of π_2^H:

$$\log PS = 0.929 + 0.732 \log Poct - 0.669\,(Mw/100) - 2.119\,\pi_2^{NOR} \quad (24)$$

(0.024) (0.000) (0.000) (0.000)

$W_{logPoct} = 0.929$ $W_{Mw} = -0.665$ $W\pi_2^{NOR} = -0.418$

$r^2 = 0.835$ r = 0.914 rcv = 0.891 s = 0.693 n = 37 F = 55.71

In this equation, rcv is the cross-validation coefficient and W is the regression coefficient obtained when the variables were scaled and centrated. The r^2 values between pairs of variables were quite acceptable: Mw/log Poct 0.453, Mw/π_2^{NOR} 0.014, and π_2^{NOR} /log Poct 0.023.

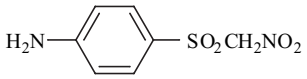

22001

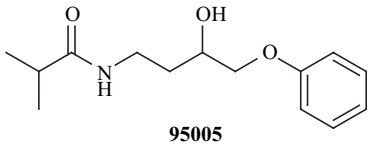

95005

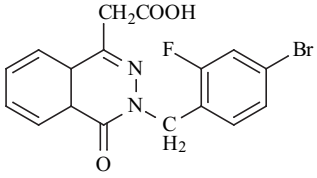

12002

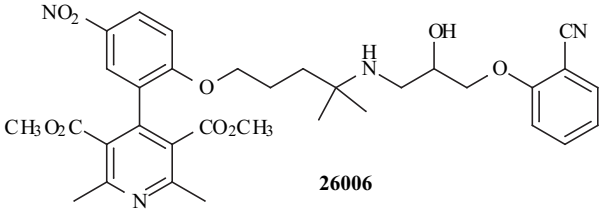

26006

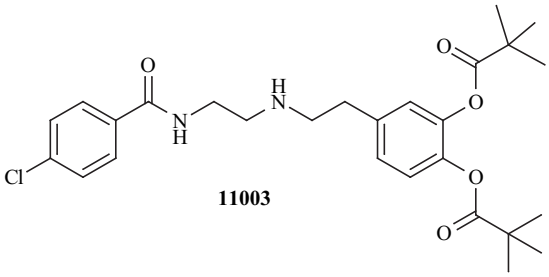

11003

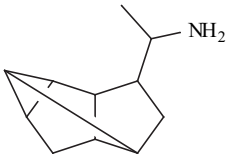

13007

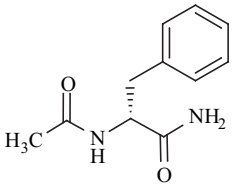

AcFNH$_2$ (I)

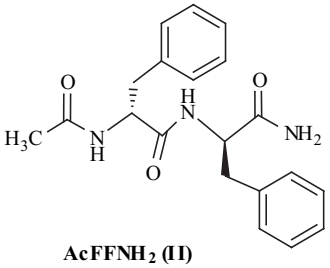

AcFFNH$_2$ (II)

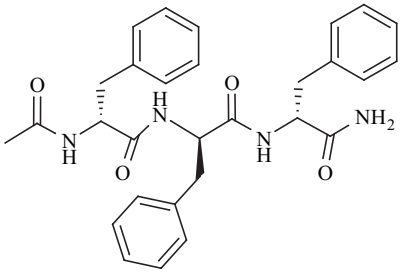

AcFFFNH$_2$ (III)

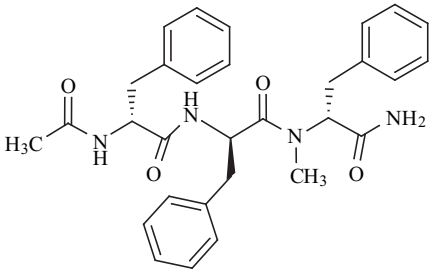

AcFF(NMeF)NH$_2$ (IV)

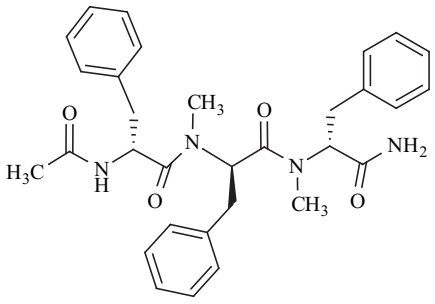

AcF(NMeF)$_2$NH$_2$ (V)

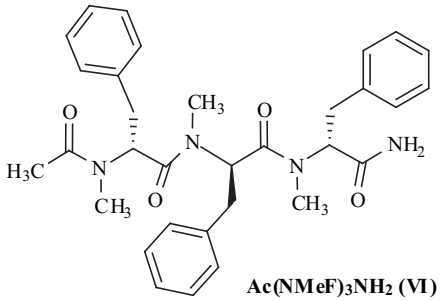

Ac(NMeF)$_3$NH$_2$ (VI)

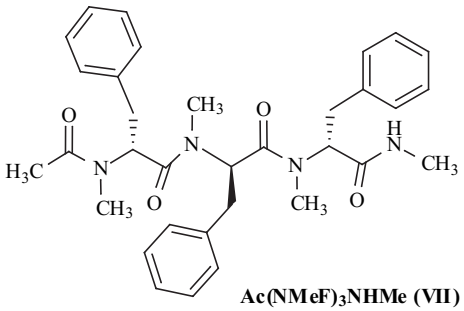

Ac(NMeF)$_3$NHMe (VII)

(Fig. 5)contd.....

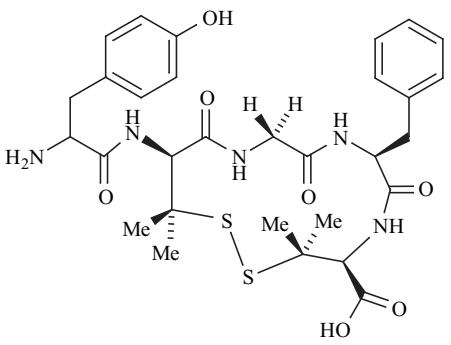

DPDPE

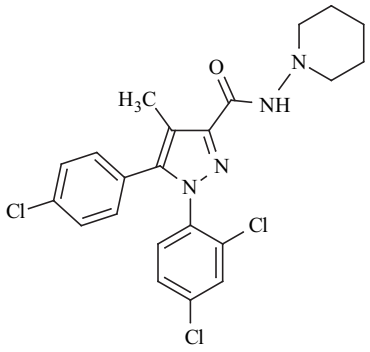

SR141716A

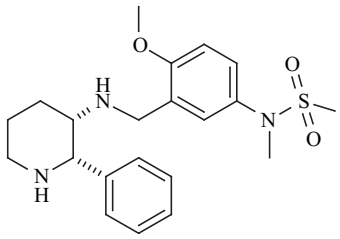

CP-141938

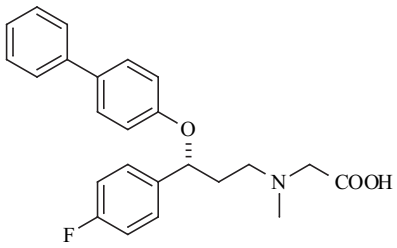

NFPS

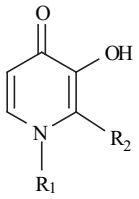

Comp.	R_1	R_2
CP20	CH_3	CH_3
CP21	CH_2CH_3	CH_3
CP24	$CH_2(CH_2)_2CH_3$	CH_3
CP29	$CH_2(CH_2)_3CH_3$	CH_3
CP25	$CH_2(CH_2)_4CH_3$	CH_3
CP94	CH_2CH_3	CH_2CH_3

Fig (5). Chemical structures of selected compounds from Table **4** and Table **5**.

To sum up, the analysis of this general equation suggests that the balance of hydrophobicity (log Poct) and polarity (π_2^{NOR}) plays a key role in the passive diffusion of solutes across the BBB, while the negative dependence of log PS on molecular size can be rationalized based on the inverse relation that exists between the diffusion coefficient of a solute and its molecular weight.

4.1.1 Modeling BBB Permeability by Using Computational Approaches

Very recently, Liu *et al.* [86] have reported the first computational approach to predict BBB permeability of 28 structurally diverse drug-like compounds. The QSAR model was based on the topological polar surface area (TPSA) developed recently by Ertl *et al.* [87], the van der Waals surface area of basic atoms (vas_base), and on the calculated octanol-water apparent distribution constant (log $D_{7.4}$). The chemical structures for some compounds are shown in Fig. (**5**), while the log PS values along with the molecular descriptors for the 28 compounds are given in Table **5**. The PS products were determined by means of the *in situ* perfusion technique using bicarbonate-buffered saline solution as perfusate. The reported equation, which was checked from the original paper, was as follows:

log PS =

$$-2.186 + 0.261 \log D_{7.4} + 0.0587 \text{ vas\_base} - 0.00906 \text{ TPSA} \quad (25)$$
$$(0.000)\ (0.000)\qquad (0.003)\qquad (0.000)$$

$r^2 = 0.749$ r = 0.865 s = 0.488 n = 23 F = 18.86

Two uptake substrates, phenylalanine and levodopa, and three Pgp substrates, CP-141938, digoxin, and quinidine, were excluded by the authors because they fit poorly into the derived equation. Besides, as pointed out by the authors, significant improvement is achieved by omitting NFPS of data set (r^2= 0.81, s = 0.434, n=22). The model proposed was shown to apply to two external data sets consisting of 12 out of the 18 compounds reported by Gratton *et al.* [79] (six partially ionized compounds at pH 7.4 were excluded) as well as 12 out of the 21 compounds reported by Murakami *et al.* [88] (nine influx and/or efflux substrates were excluded). In addition, they found poor correlations between the log PS and the screened lipophilicity parameters, such as log Poct, log $D_{7.4}$, and the function log ($D_{7.4}$ $Mw^{-0.5}$).

In reevaluating their work we were able to obtain the following equation based on the log Poct and Mw parameters:

$$\log PS = -2.060 + 0.448 \log \text{Poct} - 0.366\ (Mw/100) \quad (26)$$
$$(0.000)\ (0.000)\qquad (0.000)$$

$r^2 = 0.797$ r = 0.893 s = 0.471 n = 22 F = 37.24

Table 5. Molecular Descriptors and Observed and Calculated log PS Values From Eq. 26 for Compounds Studied by Liu *et al.* [86]

Compound	LogPS Oberved(a)	LogPS Calculated(b)	MW	LogPoct	Log(7.4)	Vsa_base	TPSA
Antipyrine	-2.0	-2.63	188.2	0.27	0.27	0	23.55
CP-141938	-3.6	-3.03	403.6	1.13	-1.26	11.37	70.67
SR141716A	-1.6	-1.60	463.8	4.82	4.81	0	50.16
Caffeine	-2.0	-2.81	194.2	-0.08	-0.08	0	58.44
Chlorambucil	-1.6	-1.52	304.2	3.7	1.13	0	40.54
Colchicine	-3.3	-3.06	399.4	1.03	1.03	0	83.09
DPDPE	-3.6	-4.10	659.8	0.84	-1.89	17.74	199.95
Daunomycin	-2.7	-2.92	527.5	2.39	0.58	17.74	185.84
Digoxin	-4.3	-4.41	781	1.14	1.14	0	203.06
Dopamine	-2.1	-2.57	153	0.12	-2.09	17.74	66.48
Fluoxetine	-1.5	-1.24	309.3	4.35	1.69	5.68	21.26
Glycine	-3.5	-3.83	75.07	-3.33	-5.83	17.74	63.32
Hypoxanthine	-3.5	-2.83	138.1	-0.59	-0.59	0	69.81
Levodopa	-1.8		197.2	-2.53	-5.04	17.74	103.78
Methotrexate	-3.9	-3.85	454.5	-0.28	-1.46	0	210.54
Morphine	-2.7	-2.54	285.3	1.27	0.46	0	52.93
NFPS	-2.9		393.5	5.34	2.84	0	49.77
Phenylalanine	-1.3		165.2	-1.19	-3.7	17.74	63.32
Phenytoin	-2.2	-1.85	252.3	2.52	2.44	0	58.2
Propranolol	-1.2	-1.62	259.4	3.09	1.34	5.68	41.49
Quinidine	-3.4		324.4	3.44	1.72	0	45.59
Salicylic acid	-3.4		138.1	2.06	-1.86	0	57.53
Taurocholic acid	-4.1	-3.48	515.7	1.04	-3.06	0	144.16
Testosterone	-1.1	-1.56	288.4	3.47	3.47	0	37.3
Theobromine	-3.0	-3.07	180.2	-0.79	-0.79	0	67.23
Theophylline	-2.9	-2.70	180.2	0.05	0.02	0	69.3
Valproic acid	-2.5		144.2	2.53	-0.02	0	37.3
Xanthine	-3.8	-2.98	152.1	-0.81	-0.81	0	86.88

(a) Observed log PS values in cm3 s-1 g-1. (b) Calculated PS values from Eq **26**.

To note that log Poct and Mw descriptors are not intercorrelated ($r^2 = 0.13$). The six removed compounds to obtain eq. **26** were phenylalanine, levodopa, quinidine (all omitted by the authors for derivation of eq. **25**), and three carboxylic compounds: NFPS, salicylic acid and valproic acid. An interesting point to highlight is the slightly worse performance that is obtained when the data point for NFPS is included in the analysis ($r^2 = 0.74$, r = 0.86, s = 0.52, n =23 and F = 28.16), but using the CLOGP value (3.99) instead of ACD-log Poct value (5.34) which was used by the authors.

The data set studied by Liu *et al.* [86] included several drugs for which a carrier-mediated transport mechanism has been identified (see Table **5**). Despite this fact, equation 26 is highly significant statistically and from a qualitative point of view, it is consistent with all the previously obtained equations. Nevertheless, a special comment is needed for the omission of salicylate and valproic acid from eq. **26**. In the case of salicylic acid, evidence suggests that its restricted brain penetration may be ascribed to efficient brain-to-plasma efflux *via* the monocarboxylic acid transport (MCT) system [89] as well as *via* other related transporters such as OAT1

and OAT2, both members of the organic anion transporter (OATs) family [24,90]. It should be noted, however, that MCT is a bidirectional transporter and has been recently reported to be involved in the brain uptake of salicylic acid and other organic anions such as benzoic acid and lactic acid [91]. A similar trend has also been observed in the case of valproic acid showing that its brain uptake is mediated by MCT, but the resulting low brain penetration observed is due to efflux transport at the BBB *via* the multidrug resistance-associated proteins (MRPs) and other organic anion transporters [92,93].

Another possible explanation for the overprediction of these carboxylic compounds comes from the work of Luco *et al*. [94], who used membrane-like systems, such as immobilized artificial membrane (IAM) chromatography, to study the chromatographic behavior of some carboxylic acids among several other compounds. It was found that the carboxylic compounds clearly form a subgroup that behaves differently in IAM chromatography. Several QSRR equations were derived suggesting that the electronic interaction between the ionized carboxyl group and the polar head-groups of phospholipids of the IAM phases was the main reason for this behavior.

4.1.2 Modeling BBB Permeability by Using Chromatographic Techniques

Reversed-phase liquid chromatography (RPLC) has been widely recognized as a valuable method to obtain lipophilicity parameters which are extensively used in studies of quantitative structure-activity relationships (QSAR) [72]. The usefulness of micellar liquid chromatography (MLC) for the prediction of drug permeation across the BBB has been reported very recently by Medina-Hernández *et al.* [73]. This technique is a mode of RPLC where micelles are used as the modifier of the aqueous mobile phase with a hydrocarbonaceous stationary phase. The authors reported a good correlation ($r^2 = 0.94$) between the logarithm of capacity factor ($\log k'_{MLC}$) in MLC (Brij35 was used as surfactant) and the BBMEC permeability coefficient for eight drugs: acyclovir, caffeine, antipyrine, propranolol, estrone, progesterone, testosterone, and haloperidol.

In addition, a reasonable correlation was reported by the authors between the BB concentration ratio and $\log k'_{MLC}$ for a data set of 44 diverse drugs including neutral, anionic, and cationic compounds:

$$\log BB = -0.87 (\pm 0.12) + 0.84 (\pm 0.08) \log k'_{MLC} \quad (27)$$

$r^2 = 0.74$ r = 0.86 s = 0.39 n = 41 F = 109.6

Three compounds were removed to obtain eq **27**: thioridazine, verapamil and indomethacine. On the basis of the derived model, the authors suggested that MLC can be used to predict the BBB permeation of drugs at an early stage of the drug discovery process.

The applicability of MLC was also reported by Fujiwara *et al.* [74]. They found good correlations (r^2 range 0.86-0.94) between the micelle/water partition coefficient (P_{mic}) and the BBB permeability data of several miscellaneous drugs. In order to understand the passive transport across the BBB from a thermodynamic point of view, the authors measured the individual hydrophobic contributions of the enthalpy and entropy terms embodied in the P_{mic} term. The parameters used to explain BBB permeability were the hydrophobic enthalpy constant (P_H) and the hydrophobic entropy constant (P_S). It was found a good correlation between P_H and BBB permeability, whereas $\log P_{mic}$ fails to do so.

On the other hand, IAM chromatography has also been successfully applied to predictions of drug permeability across several biological barriers such as human skin, intestinal epithelium, epithelial Caco-2 cell line and the BB barrier (for a recent review see [95]). Thus, Reichel and Begley [96] observed good correlations between log BUI and the $\log k_{iam}$ for a group of six hydrophobic steroids and six hydrophilic biogenic amines (r^2 range 0.729 to 0.747, respectively).

Moreover, the ability of IAM chromatography to predict the BB concentration ratio was also demonstrated by Salminen *et al.* [97]. They used a set of 26 compounds containing acidic, neutral, and basic functionalities to evaluate the relationship between the $\log k_{iam}$ and the log BB ratio. By omitting five outliers (cimetidine, indomethacin, ranitidine, salicylic acid, and thioridazine), a reasonable equation was obtained by the authors when $\log k_{iam}$ and molecular volume (V_m) were used as descriptor variables:

$$\log BB = 1.28 + 0.58 \log k_{iam} + 0.89 I_2 - 0.01 V_m \quad (28)$$

$r^2 = 0.848$ r = 0.921 s = 0.27 n = 21 F = 31.5

I_2 is an indicator variable that takes the value of 1 or 0 for the presence or absence of amino-nitrogen in the molecule. The omission of the outliers may be justified because an active transport mechanism has been identified for these compounds. For example, cimetidine, indomethacin, ranitidine, and thioridazine are Pgp substrates, whereas salicylic acid and cimetidine are known efflux substrates *via* OATs transporters [24,90].

Very recently, Péhourcq *et al.* [134] also investigated the suitability of IAM chromatography to predict the diffusion of arylpropionate non-steroidal anti-inflammatory drugs into the cerebrospinal fluid (CSF). The influence of molecular weight and the dissociation constant (pKa) were also studied. A reasonable equation was obtained by the authors between the $AUC_{CSF} : AUC_{(free\ plasma)}$ ratios (R_{AUC}) and the $\log k_{iam}$ of the eight arylpropionic acids studied:

$$\log (R_{AUC}) = -7.82 (1.40) (\log k_{iam})^2 + 21.57(3.88) \log k_{iam} - 14.09 \quad (29)$$

r = 0.928 s = 0.20 n = 8 F = 15.6

The inclusion of MW in eq. 29 improved the fit slightly, whereas pKa did not influence the fit of the parabolic equation. The reported models suggest that diffusion of NSAIDs into the CSF depends primarily on the lipophilicity and Mw of the compounds under study.

A more complex measure of brain penetration was used by Ducarme *et al.* [98] to evaluate the relationship between the $\log k_{iam}$ and the BBB transport of fifteen 1,3,5-triazines possessing CNS activity. It was shown by the authors that the potentiation of oxotremorine-induced tremors, which was determined by using an *in vivo* mouse model, correlated well

with the log k_{iam} parameter in a parabolic model ($r^2 = 0.77$, s= 0.31, n=15 and F= 20).

4.2 QSAR MODELS BASED ON BB DISTRIBUTION DATA

The majority of brain permeation QSAR models have been based on measures of Brain/blood distribution at or near the steady state. In contrast to the correlations obtained with log PS, the log Poct and Mw parameters have shown a limited performance in predicting brain/blood concentration ratios (log BB). However, as already discussed in section 3.1, log BB is a composite parameter since several factors unrelated to membrane permeability influence the final drug concentration in the brain; and therefore, it is not an appropriate index of BBB permeability [36].

In this review, we have focused on the recent progress that has been made on modeling of log BB data, since the BB-QSAR models reported during the period 1988s-2002 have already been recently reviewed by Norinder and Heaberlein [21], Sippl [31], Clark [20], Ecker and Noe [19], and others [22,29,30]. However, it seems appropriate to show a summary of QSAR models developed during this period in order to compare the results with the work that has been recently done in this area. A summary of the models developed in the period 1988-2002 is provide in Table **6**. The log BB values for 157 structurally diverse compounds and the corresponding structures may be taken from Sippl [31] and Platts and Abraham [113].

In the period 2003-2004, several log BB QSAR models were reported based on Abraham's data set [113] (n = 148), and using physicochemical, topological and molecular orbital calculations for prediction of log BB values. For instance, Hutter [122] studied the relationship between the log BB for a training set of 90 compounds and several descriptors derived from AM1 calculations. The reported equation including 12 descriptor variables was as follows:

$$\log BB = 3.50 + 0.0449\ (\pm 0.0089)\ M\text{-}ESP - 0.0096\ (\pm 0.0027)\ VXBAL - 0.3723\ (\pm 0.0516)\ HBDON$$
$$+ 0.0181\ (\pm 0.0074)\ CHBBA + 0.0948\ (\pm 0.0287)\ HALO + 0.4456\ (\pm 0.1623)\ NO2 + 0.2148\ (\pm 0.1215)\ SU$$
$$- 0.0927\ (\pm 0.0626)\ AR6 - 0.2457\ (\pm 0.0552)\ IP + 0.1170\ (\pm 0.0253)\ PCGA$$
$$- 0.0205\ (\pm 0.0066)\ PCGC - 0.0395\ (\pm 0.0182)\ ROTB$$
$$r^2 = 0.865\ r = 0.930\ s = 0.309\ n = 90\ F = 41.125 \qquad (30)$$

where the *M-ESP* and *VXBAL* variables are the mean electrostatic potential and the product of the balance parameter and the total variance of ESP, respectively. Both variables express the polarity of the molecular surface, whereas the *HBDON* and *CHBBA* variables correspond to the hydrogen-bond donor/acceptor capabilities of the compounds. The *HALO*, *SU*, *NO2*, and *AR6* variables indicate the presence of certain chemical groups in the molecule, such as halogen and sulfur atoms, nitro groups and aromatic 6-membered rings, respectively. Finally, the *IP* term is the ionization potential and the *PCGs* terms are geometrical descriptors derived from AM1-optimized 3D geometry of the molecule. The predictive ability of eq. **30** was evaluated for a set of 23 diverse compounds giving a mean absolute error of 0.566 and a standard deviation of 0.671. To summarize, eq. **30** shows that both polar surface area and hydrogen bonding influence BBB permeability negatively, whereas the *PCGA* and *PCGC* descriptors suggest that spherical-shaped molecules will be favored to cross the BB barrier. In addition, the *ROTB* descriptor quantifies the number of rotatable bonds in the molecule and their negative coefficient in eq. **30** indicates a detrimental effect of the molecular flexibility on BB distribution.

A similar study was performed by Subramanian *et al.* [123], who related log BB for a training set of 58 compounds to several topological descriptors and 3D structural parameters by using genetic partial least-squares (G/PLS) modeling. The following 3-component model based on seven molecular descriptors was reported:

$$\log BB = - 0.0204 + 0.122\ SsssN - 0.114\ ROTB + 0.0359\ Jurs\text{-}WNSA3 - 0.0615\ SdsN + 0.313\ AlogP$$
$$- 0.0959\ SsssCH + 0.108\ Rog$$
$$r^2 = 0.845\ r = 0.919\ s = 0.308\ n = 58\ F = 97.9 \qquad (31)$$

where the *SsssN*, *SdsN*, and *SsssCH* descriptors are the electrotopological indexes of specified atom types, *AlogP* is the Ghose and Crippen log Poct, *Jurs-WNSA3* is the surface weighted charged partial surface area and *Rog* is the radius of gyration of the molecule. The predictive ability of the model was evaluated for a set of 39 diverse compounds giving a reasonable standard deviation (s= 0.463). The derived PLS model suggests that log BB depends positively on hydrophobic and geometrical factors, while the conformational flexibility (*ROTB*) and the molecular polarity have the opposite effect.

In contrast to the models based on 3D parameters, Hou and Xu [124] proposed the correlation between log BB and 2D descriptors only, as shown in the following equation:

$$\log BB = 0.1256 + 0.160\ Slog\ P - 0.0133\ HCTPSA - 0.0148\ <Mw - 360> \qquad (32)$$
$$r^2 = 0.743\ r = 0.862\ s = 0.375\ n = 78\ F = 66.9$$

where HCTPSA is the high-charged topological polar surface area calculated from the contributions related to the 2D topological information and the Gasteiger partial atomic charges, and SlogP refers to partition coefficient octanol-water calculated by using an extensively reparametrized variety of the SLOGP program. The <Mw–360> variable is the excessive molecular weight which is equal to zero if the <Mw-360> is negative; otherwise, it is equal to <Mw-360> value. Hou's model showed a good predictivity for two external test sets (s equal to 0.26 and 0.48 for 13 and 22 compounds, respectively) and due to the fact that it is only based on 2D structures, the model can be used for high-throughput screening of large compound libraries. Finally, the negative coefficient of <Mw–360> in eq. **32** supports the hypothesis of the molecular weight threshold at BBB and interestingly, this is in agreement with the results reported by Liu *et al.* [114] (see Table **6**).

In a very recent study, Stanton *et al.* [125] introduced a new series of whole-molecule molecular structure descriptors, termed hydrophobic surface area or *HAS* descriptors, with the aim of obtaining information related to

Table 6. Summary of Log BB QSAR Models Reported in the Period 1988s-2002

Author	n	r	s	Descriptors	Predictive Performance
Young [99]	20	0.831	0.439	Seiler's Δ logP parameter	nr
van de Waterbeemd [100]	20	0.943	0.290	Δalk and Vm	nr
Calder [101]	25	0.730	nr	Seiler's ΔlogP parameter	nr
Abraham [102,103]	57	0.952	0.197	Solvation parameters	s = 0.14, n = 5
Kaliszan [68]	20	0.943	0.271	logPcyh and Vwav	nr
Kaliszan [68]	33	0.947	0.126	logPoct and Mw	nr
Lombardo [104]	55	0.82	0.41	ΔGw	s = 0.55, n = 6
Salminen [97]	23	0.921	0.32	logPoct, Vm and I_3 (dummy variable)	nr
Norinder [105]	56	0.913	0.312	PLS, 14 MolSurf descriptors	s = 0.55, n = 6
Luco [106]	58	0.922	0.318	PLS, 18 topological indexes	s = 0.37, n = 37
Clark [107]	55	0.887	0.354	PSA and ClogPoct	s = 0.20, n = 10
Kelder [108]	45	0.917	0.36	Dynamic PSA	nr
Segarra [109]	20	0.850	0.416	Grid calculations Surface of water probe map at –2 Kcall (S_2_W)	nr
Feher [110]	61	0.854	0.424	ACD-logPoct, PSA and HBA	s = 0.76, n = 14 s = 0.80, n = 25
Osterberg [111]	69	0.869	0.378	HBAo, HBAn, HBD, and ACD-logPoct	nr
Osterberg [111]	45	0.871	0.452	HBAo, HBAn, HBD	nr
Ertl [87]	57	0.812	nr	TPSA (topological PSA)	Nr
Kersdti [112]	55	0.85	0.37	Gsolv	s = 0.14, n = 5 s = 0.37, n = 25
Platts and Abraham [113]	148	0.863	0.343	Solvation parameters and Icooh (dummy variable)	s = 0.38, n = 74
Liu [114]	55	0.888	0.35	Lipoaffinity descriptor based on E-state indexes (LA) and Mw	nr
Liu [114]	55	0.833	0.42	TPSA	nr
Jorgensen [115]	105	0.876	nr	Atom-type weighted water-accessible surface areas (ATW WASA)	nr
Klamt [116]	65	0.883	0.43	COSMO-RS descriptors (area, sig2, sig3, hbacc and hbdon)	nr
Kaznessis [117]	76	0.958	0.203	HABC, Mvol and SASA descriptors derived from monte Carlo Simulations In water	s = 0.48, n = 4
Hall [118]	102	0.812	0.45	E-state indexes, HS^T (hydrogen bond donors), HS^T (arom) and Δchi2v	s = 0.38, n = 20
Testa [119]	79	0.883	nr	VolSurf descriptors	q^2 = 0.65 (training set)
Hopfinger [120]	56	0.919	nr	PSA, ClogPoct and membrane-interaction descriptors	s = 0.39, n = 7
Lobell [121]	48	0.915	0.19	TPSA, Pos charge, Neg Charge, Shadow-nu (geometrical descriptor) and ΔGdesolv (oct-water)	s = 0.41, n = 17

the structural features responsible for hydrophobic and hydrophilic intermolecular interactions. Applying these new descriptors to the study of the blood-brain barrier penetration for a training set of 97 compounds (included in the 106-compound data set used by Rose *et al.* [118]) yielded the following regression equation:

$$\log BB = 0.534\ (0.07) + 0.044\ (0.007)\ WNSA\text{-}3 + 0.244\ (0.034)\ V4P - 0.132\ (0.026)\ NDB + 0.030\ (0.004)\ PNHS\text{-}3 \quad (33)$$

$r^2 = 0.778$ r = 0.882 s = 0.375 n = 97 F = 80.7

where WNSA-3 is the negatively charged weighted solvent accessible surface area, V4P is the valence-corrected fourth-order path molecular connectivity index, NDB corresponds to the number of double bonds in the molecule, and PNHS-3 is a *HAS* descriptor that is calculated from the atomic constant weighted by the total hydrophilic surface area (Σ (*-Ai)*(-log *Pi*)). A PLS analysis was used by the authors to extract the physical interpretation of eq. **33**. These results showed that small hydrophobic molecules are favored for BB penetration over large hydrophilic molecules.

An alternative methodology for the prediction of BBB penetration as well as other physicochemical properties was introduced by Sun [126]. The method was based on generic molecular descriptors calculated from an atom type classification system by using the Daylight Chemical Information System. In all, 218 atom types were identified and their contributions to different target properties were obtained by using the partial least squares (PLS) method. For the log BB prediction, Abraham data set of 57 compounds [102] was selected as the training set and the PLS analysis resulted in a significant three-component model with the following statistics: r^2 of 0.897, r of 0.947, s of 0.259 and q2 of 0.504. However, the predictive ability of the model was not very good, mainly due to the still scarce information of log BB values available in the literature.

An interesting topological approach for prediction of log BB values was recently employed by Cabrera *et al.* [127]; it is based on the calculation of the spectral moments of the so-called topological bond matrix. The approach is called TOPS-MODE (topological substructural molecular design approach) and has been successfully applied to different QSPR and QSAR studies [128]. A data set of 123 compounds, which was based on Abraham's data set [113], was used to obtain the log BB-regression model. The best regression equation found for the full data set was as follows:

$$\log BB = -0.032\ (\pm 0.005) - 0.046 \times 10^{-3}\ (\pm 0.003)\ \mu_1^{PS}.\mu_1^{AM} + 0.227\ (\pm 0.025)\ \mu_1^{H} \quad (34)$$

$r^2 = 0.697$ r = 0.835 s = 0.422 n = 114 F = 127.78

where the variables used are related to polar surface (μ_1^{PS}), atomic mass (μ_1^{AM}) and the hydrophobicity (μ_1^{H}) of the compounds. The predictive ability of the model was reasonable, and an important aspect to point out about the obtained model is the possibility of obtaining the qualitative contribution of any kind of substructure to the blood-brain partitioning, which can be of interest to design novel drug candidates.

A different approach for prediction of log BB values was very recently introduced by the group of Hopfinger *et al.* [129]. The methodology proposed is based on the fact that all compounds in a structurally diverse data set may not interact with the blood-brain "membrane" in the same manner. Thus, according to the authors, the general BB-QSAR models reflect only an average picture of several drug-membrane interactions involved in the BBB penetration of each subset of compounds included in the general data set. In order to address this mechanistic problem, the authors proposed a new method by using a combination of 4-D-molecular similarity measures and cluster analysis to construct optimum BB-QSAR models. The compounds were characterized by both, two-dimensional and three-dimensional membrane-interaction QSAR descriptors. The general QSAR model obtained for the complete 150 compound data set was as follows:

$$\log BB = 0.064 - 0.01\ TPSA + 0.20\ CLOGP$$

$r^2 = 0.69$ r = 0.831 rcv = 0.774 n = 150 (35)

Afterwards, the general data set was divided into subsets based on 4D-molecular similarity measures using cluster analysis and several QSAR models were constructed for each cluster subset. The obtained results showed that the specific properties governing BBB permeability vary across chemically diverse compounds.

Another way to evaluate BBB permeation has been the use of artificial neural networks since they are robust methods that frequently render the possibility of obtaining fast and accurate predictions. Thus, Winkler and Burden [130-131] reported the use of Bayesian neural nets for modeling the BBB partitioning of 106 compounds employing three types of molecular descriptors: (i) property based descriptors (number of hydrogen bond donors, acceptors, rotatable bonds, log Poct, MW and PSA); (ii) topological indexes and (iii) descriptors based on eigenvalues of modified adjacency matrices and atomic charges binned into fingerprints. The models based on property based descriptors showed the best performance with the value of r and s within the range of 0.63-0.81 and 0.37-0.50, respectively. In addition, the models indicated that the most relevant molecular properties were related to hydrophobic, hydrogen bond and structural flexibility properties; similar conclusions were arrived at by other models found in the literature. Dorronsoro *et al.* [132] also used neural network models to predict the BBB permeability of 36 different drugs. The goal of their study was to evaluate the suitability of several descriptors generated by a novel program, called CODES, which codifies the molecules from a topological point of view. Though a reasonable model was obtained (r = 0.94), the robustness and predictivity of CODES model should be evaluated by applying it to larger sets of compounds. Another similar study was reported by Fu *et al.* [133]. They proposed a neural network model by using the back-propagation algorithm and several quantum chemical descriptors to predict the BBB permeability of 56 different compounds. The model obtained was suitable for the training set, with a RMSE of 0.236, but it should be noted that the test set (5 compounds) was based on too small a number of data points.

Finally, a QSAR study to evaluate the BBB permeability of eight potential neuroprotective agents was recently reported by Zah *et al.* [135]. The compounds, eight polycyclic undecyl amines, were synthesized and were characterized by both, experimental and calculative methods, followed by determination of brain partitioning data for each test compound. The results obtained established the

significance of lipophilicity with regard to the BBB permeability of these polycyclic amines.

4.3 QSAR MODELS BASED ON QUALITATIVE BRAIN PENETRATION DATA

Another way to predict BBB penetration has been the application of classification methods which are generally based on observations of CNS activity/inactivity. Some authors; however, have also used the log BB data by defining a cut-off log BB value above which the drug is classified as CNS^+ and below which it is classified as CNS^-.

An early study of this type was carried out by Seelig *et al.* [136]. Twenty-eight drugs were selected and classified according to the CNS availability by means of their surface activity, which was determined by using the corresponding Gibbs adsorption isotherms in terms of (i) the onset of surface activity (Co), (ii) the critical micelle concentration (CMC), and (iii) the surface area at the air/water interface. The study showed that the CNS^- compounds are either not surface active, very hydrophobic with low Co and CMC values, or relatively hydrophilic with high Co and CMC values. On the other hand, compounds which do cross the BBB exhibit intermediate Co and CMC values and have cross-sectional areas which are smaller than those of a membrane lipid molecule. Very recently, Suomalainen *et al.* [137] reported a similar approach based on a novel *in vitro* platform surface activity profiling to distinguish between CNS and non CNS drugs. Interfacial partitioning coefficient, cross-sectional area, and CMC were derived from Gibbs adsorption isotherms available for 76 structurally diverse drugs. As an approximation for the membrane partitioning coefficient, the K_{memb} constant was derived for the analyzed compounds and the plot between the *in vivo* permeability data and log K_{memb} allowed to obtain a good classification between the compounds with CNS activity/inactivity. A drawback of this proposed methodology is the lack of surface activity data for a large set of compounds.

A different classification approach based on several physicochemical parameters was conducted by van de Waterbeemd *et al.* [138]. It was demonstrated by the authors that both H-bonding and molecular size descriptors can be used as suitable descriptors for classifying the CNS activity/inactivity of drugs. Thus, for the 125 CNS^+/CNS^- compounds studied, the authors concluded that for brain penetration the compounds should have a MW< 450 and PSA < 90Å^2. Following a similar line of analysis, and taking into account the strong correlation that exists between the number of nitrogen and oxygen atoms (N+O) in a molecule and the corresponding PSA value, Norinder and Haeberlein [21] proposed a very simple BBB classification system based on two rules: (i) if the (N+O) value is five or less in a molecule, it has a high chance of entering the brain, and (ii) if [log Poct – (N+O)] is >0, then log BB is positive. The proposed classification system showed a good predictive quality on several BBB data sets (>90% accuracy).

More recently, other empirical approaches have been applied to sets of CNS active/inactive compounds. Thus, Di *et al.* [139] reported the development of a modified parallel artificial membrane permeability assay (PAMPA), which was firstly introduced by Kansy *et al.* [140] as a high throughput permeability assay to predict oral absorption. In order to improve the prediction of BBB penetration, Di *et al.* [139] used porcine brain lipids for method development and the assay was applied to a set of 30 structurally diverse drugs. The method was validated with 14 Wyeth Research compounds with a high success and throughput; however, their application to more large sets of compounds will show the real predictive ability of the proposed method. Another empirical model for predicting the BBB penetration of 63 CNS^+/CNS^- compounds was proposed by Gulyaeva *et al.* [141]. The method was based on the analysis of the relative hydrophobicity and lipophilicity of the compounds. Thus, the combination of these two parameters; that is, the relative hydrophobicity estimates ($N_{[CH2]}$) obtained by aqueous two-phase partitioning (water/dextran-polyethylene glycol) and the lipophilicity measured by octanol-buffer partitioning and RPLC techniques, allowed to make an adequate differentiation between the analyzed CNS^+/CNS^- compounds. The main drawback of the methodology proposed is that the experimental determination of partition coefficients is very laborious and time-consuming.

Finally, a new empirical model for predicting the BBB penetration of 93 marketed drugs was proposed by Doan *et al.* [142]. The method was based on the determination of *in vitro* BBB permeability (MDCK cell lines were used), P-glycoprotein substrate profiles, and several physicochemical properties for 48 CNS and 45 non-CNS therapeutic agents. The results showed that permeability, Pgp-mediated efflux, and certain physicochemical properties are factors that can differentiate between the CNS and non-CNS drugs. Analysis of physicochemical properties revealed that the CNS drug set had fewer hydrogen bond donors, fewer positive charges, greater lipophilicity, lower polar surface area, and reduced flexibility compared with the non-CNS group ($p<0.05$).

The first nonempirical approach used for classification purposes was conducted by Basak *et al.* [143]. They applied a discriminant analysis to the same data set used by Seelig *et al.* [136], but using several nonempirical descriptors including topological indexes (TIs), a hydrogen bonding descriptor(HB1) and CLOGP. Three QSAR models were constructed, having 100% accuracy for classifying the CNS^+ compounds and 91.75% accuracy for the CNS^- compounds. Interestingly, all the models contained the HB1 parameter and four or five TIs, but CLOGP was not selected as a variable during the selection process indicating that lipophilicity was not a reliable parameter for classifying the CNS activity of this data set.

Very recently, another topological model was reported by Cabrera *et al.* [144] by using the TOPS-MODE approach to classify 302 CNS and non-CNS compounds. A discriminant analysis was also used and the obtained discriminant function classified correctly the 83.33% of drugs with CNS activity in the training set and the 80.26% of inactive compounds, for a good global classification of 81.79%. It was demonstrated by the authors that hydrophobicity increases CNS activity, while the dipole moment and the polar surface area decrease it; evidencing the capacity of the TOPS-MODE descriptors to estimate CNS activity for new drug candidates.

A different nonempirical approach based on 3D molecular descriptors was reported by Crivori *et al.* [145] for a BBB-classification model by using principal component analysis (PCA) of a large number of descriptors obtained by the VolSurf program. The molecular descriptors, such as total volume, total surface, globularity, electrostatic and lipophilicity potentials etc., were calculated using 3D molecular interaction fields against several probe atoms. A qualitative PCA model was obtained by using 72 VolSurf descriptors for a training set of 44 compounds, which was able to separate CNS^+ from CNS^- compounds in a scatter plot of the first two principal components. Using a test set of 120 compounds, the model was able to correctly classify 90% of the CNS^+ compounds and about 65% of the CNS^- compounds.

More recently, Wolohan and Clark [146] developed a 3D classification method which combined molecular interaction fields with the soft independent modeling of class analogy (SIMCA) to predict BBB permeation for a training set of 55 compounds. The CoMFA (Comparative Molecular Field Analysis) steric and electrostatic fields produced the best model, which was able to correctly classify 98% of the compounds for each one of four selected categories. In addition, for the four test sets randomly selected from the BBB data, an average of 81% of drugs were correctly predicted. It should be noted, however, that the 3D-methods mentioned above are highly conformation dependent and as such offer limited applicability for virtual screening of large compound libraries.

Several authors have used machine-learning algorithms for classifying CNS activity or inactivity of drugs. For instance, Ajay *et al.* [147] reported the use of Bayesian neural nets to distinguish between a very large set of CNS^+ and CNS^- compounds; that is, 15000 actives and over 50000 inactives. The compounds were selected from the Comprehensive Medicinal Chemistry and MACCS-II Drug Data Report drug databases based on whether they were described as having some kind of CNS activity in the databases. The developed model correctly predicted 83% of active compounds (CNS^+) and 79% of the inactive ones (CNS^-), when the compounds were described by seven 1D descriptors (log Poct, MW, number of hydrogen bond donors and acceptors, etc.) and 166 2D descriptors (presence/absence of functional groups). The procedure is fast and can be applied to large data sets or virtual libraries.

Another virtual high throughput screening method to identify potentially CNS-active drugs has been reported by Keresû *et al.* [148]. In their work, a feedforward neural network was trained on 7000 compounds taken from CPS (Cipsline from Prous Science) and CDSA (Chemical Directory from Sigma-Aldrich) databases. Molecular structures were represented using 2D Unity fingerprints, and the developed model was able to correctly classify 92% and 87% of the CPS and CDSA compounds, respectively. Next, the parameterized network was validated by using a test set preselected from the CPS database, and also by the prediction of activity of compounds available in the Medchem database, having 89% accuracy for classifying the CNS-active compounds in these test set.

A most recent development in this type of approach has been reported by Doniger *et al.* [149]. In this work, two different machine-learning algorithms have been used to predict the BBB penetration of 324 CNS and non-CNS compounds. Both algorithms, the multilayered bakpropagation neural network and the support vector machine (SVM), were trained on the same data set with several molecular descriptors such as MW, log Poct, hydrogen bonding, and others variables that govern the transport across the BBB. Based on over 30 different validation sets, the SVM was able to correctly classify the CNS-activity of the compounds with an 81.5% of average accuracy, whereas the neural network showed an average performance of 75.7% with the same 30 test sets. Thus, according to the authors, the SVM algorithms outperform the neural networks because they have faster training times, and most importantly, they appear to be better able to classify small data sets.

Another different approach to the prediction of CNS activity has been recently described by Engkvist *et al.* [150]. In this work, a neural network model and a new algorithm called SUBSTRUCT, which is based on substructural analysis, have been used to predict the BBB penetration of 3678 CNS and 5000 non-CNS compounds extracted from the World Drug Index (WDI) database. For the substructural analysis by means of SUBSTRUCT classification algorithm, the molecules of both data sets (CNS^+/CNS^-) were fragmented into all possible fragments and the frequency profiles of the two data sets were calculated and compared to each other. The neural network model correctly predicted 82.5% of actives compounds (CNS^+) and the 76.5% of the inactive ones (CNS^-), whereas a comparable classification result was obtained by the SUBSTRUCT model with a prediction accuracy of 83.3% and 71.2% for the CNS^+ and CNS^- compounds, respectively. Nevertheless, in comparison with the neural network model, the SUBSTRUCT classification models do not have training times, and most importantly, their results are easy to interpret.

Finally, a very recent study carried out by Adenot and Lahana [151] is worth-mentioning. In this study, a large and diverse range of drugs (about 1700) extracted from the WDI database was modeled using discriminat analysis (DA) and PLS-DA employing a large combination of molecular descriptors such as surface areas, electronic and topological parameters, and several molecular properties. The objective of the study was to identify CNS drugs by constructing QSAR models that discriminate between potential 1336 CNS and 259 non-CNS drugs including 91 P-glycoprotein substrates (either CNS^+/CNS^-). All compounds were characterized by a passive diffusion component and a P-gp efflux component. Thus, three categories of explanatory variables (BBB_{pred}, C_{diff}, PGP_{pred}) were suggested to express the level of permeation of the analyzed compounds. The permeation score C_{diff} reflects the level of permeation directly from five permeation components (Mw<500, ClogP<5, H-bond donor<= 5, H-bond acceptor <=10 and molecular polar surface) onto a unique continuous scale. On the other hand, BBB_{pred} and PGP_{pred} are the corresponding discriminant functions obtained. Thus, a CNS drug mapping using both, PGP_{pred} *vs.* C_{diff}, and PGP_{pred} *vs.* BBB_{pred}, was proposed as a tool for CNS drug virtual screening.

4.4 QSAR MODELS AND BBB TRANSPORT SYSTEMS

Factors that influence brain concentrations of drugs include the rate of BBB permeability by passive diffusion, metabolic stability, and active transport out of the brain by efflux mechanisms. As mentioned in the introduction, an increasing number of efflux transporters have been identified in the endothelial cells that form the BBB, such as the multidrug resistance transporters (P-gp, MRPs, BCRP), the organic ion transporters (OATPs and OATs), and the monocarboxylic acid transporters. However, P-gp, some of the MRPs and BCRP are strongly expressed in the BBB and therefore, they play a predominant role in the bioavailability of several CNS-compounds [23-25, 32-33].

It should be noted, however, that most of the BBB-QSAR models developed so far do not take into account the multiple mechanism phenomena, which are indeed the main cause why many data points are outliers in the models derived. Thus, in our view, robust QSAR models should be developed for dealing with the multiple mechanism problem. One way would be to construct QSAR models based on data set constituted by structurally diverse drugs subject only to passive membrane permeability. Thus, more and better quality of this type of data are needed since a wide and specific coverage of chemical space would permit to create robust QSAR models. However, the determination of such permeability data is not a simple task, since in most cases the BBB permeability of drugs is due to the summation of two permeation mechanisms, that is, efflux transport and passive diffusion. This fact can be illustrated from the recently reported study by Doran *et al.* [152]. In this work, 34 structurally diverse CNS active drugs and 8 non-CNS drugs were measured in brain, plasma, and cerebrospinal fluid in the P-gp *mdr1a/1b* knockout mouse model developed by Schinkel *et al.* [153], after subcutaneous administration. The results showed that for the 34 CNS-active drugs, only seven were not affected by the P-gp, whereas all non-CNS drugs showed some degree of interaction with the P-gp.

Another way to address the multiple mechanism phenomena is to achieve a better understanding of the factors which govern the drug-transporter interactions, which would require a separate QSAR model for each one of active transport system present at BBB. Thus, over the last decade, several authors have developed comprehensive studies on structure-activity relationships for distinct classes of transporters, mainly for P-glycoprotein efflux system. However, the existence of several drug-binding sites on P-gp as well as their very wide specificity for the substrates or modulators, still present an important challenge for *in silico* models of brain permeation. Several excellent and extensive reviews on the modeling of active transport systems have been recently published and the reader is referred to these works for detailed information [154-160].

5. CONCLUSIONS

The following conclusions can be drawn from studies conducted on *in vitro* and *in-silico* BBB models.

(1) There are different *in vitro* cell-based BBB models available: those based on primary or passaged cultures of brain microvessel endothelial cells (BMEC), as well as the ones based on immortalized brain endothelial cell lines; however, the model based on brain endothelial cell lines derived from transgenic animals developed recently by Terasaki *et al.* [46], appear to be a useful and promising *in vitro* BBB model for the study of drug transport across the BBB.

(2) Most developed QSAR models based on kinetic measures of brain uptake show that lipophilicity and molecular size are the key factors regulating the entry of compounds into the CNS. In addition, we have developed a simple and robust QSAR model ($r = 0.914$, $s = 0.693$) based on a log PS data set of 37 compounds by using three molecular descriptors: log Poct, *Mw*, and π_2^{NOR}. The analysis of this general model suggests that the balance of hydrophobicity (log Poct) and polarity (π_2^{NOR}) plays a key role in the passive diffusion of solutes across the BBB, while the negative dependence of log PS on the molecular size can be rationalized based on the inverse relation that exists between the diffusion coefficient of a solute and its molecular weight.

(3) The recently developed QSAR models based on both, log BB data or qualitative brain penetration data showed good predictive abilities with respect to internal validation data set as well as to several external validation procedures. Many insights into the effects on lipophilicity, hydrogen bonding, molecular size and polar surface area have been made; however, further investigation needs to be conducted into the effects of molecular shape and flexibility and particularly charge.

(4) Finally, another major challenge on BB-QSAR modeling is the multiple mechanism phenomenon. As outlined above, BBB permeability for a majority of drugs is the result from a multiplicity of interactions between the permeant compounds and many different biological constituents at the brain endothelial cell, such as transporter proteins and membranes. Thus, robust QSAR models should be developed for dealing with this phenomenon.

ACKNOWLEDGEMENTS

The present review was supported by grants from University of San Luis and CONICET, Argentine. We wish to thank María Victoria Luco, Juan's seven-year old daughter, her friendly support.

REFERENCES

[1] Li, A.P. *Drug Discov. Today*, **2001**, *6*, 357.
[2] Di, L.; Kerns, E.H. *Curr. Opin. Chem. Biol.*, **2003**, *7*, 402.
[3] Lin, II.J.; L.U, A.Y.II. *Pharmacol. Rev.*, **1997**, *49*, 403.
[4] Smith, D.A.; Van de Waterbeemd, H. *Curr. Opin. Chem. Biol.,* **1999**, *3*, 373.
[5] Van de Waterbeemd, H.; Smith, D.A.; Beaumont, K.; Walker, D.K. *J. Med. Chem.*, **2001**, *44*, 1.
[6] Fujita, T. *Quant. Struct.-Act. Relat.*, **1997**, *16*, 107.
[7] Seydel, J.K.; Schaper, K.J. *Pharmac. Ther.,* **1982**, *15*, 131.
[8] Lien, E.J. *Ann. Rev. Pharmacol. Toxicol.,* **1981**, 21, 31.

[9] Ekins, S.; Waller, C.L.; Swaan, P.W.; Cruciani, G.; Wrighton, S.A.; Wikel, J.H. *J. Pharmacol. Toxicol. Method,* **2000**, *44*, 251.

[10] Walters, W.P.; Murcko, M.A. *Adv. Drug Deliv. Rev.,* **2002**, *54*, 255.

[11] Jorgensen, W.L.; Duffy, E.M. *Adv. Drug Deliv. Rev.,* **2002**, *54*, 355.

[12] Groot, M.J.; Ekins, S. *Adv. Drug Deliv. Rev.,* **2002**, *54*, 367.

[13] Kirton, S.W.; Baxter, C.A.; Sutcliffe, M.J. *Adv. Drug Deliv. Rev.,* **2002**, *54*, 385.

[14] Van de Waterbeemd, H.; Eric, G. *Nat. Rev. Drug Discov.,* **2003**, *2*, 192.

[15] Hansch, C.; Leo, A.; Mekapati, S.B.; Kurup, A. *Bioorg. Med. Chem.,* **2004**, *12*, 3391.

[16] Hansch, C.; Mekapati, S.B.; Kurup, A.; Verma, R.P. *Drug Metab. Rev.,* **2004**, *36*, 105.

[17] Mälkiä, A.; Murtomäki, L.; Urtti, A.; Kontturi, K. *Eur. J. Pharm. Sci.,* **2004**, *23*, 13.

[18] Greig, N. H.; Brossi, A.; Pei, X. F.; Ingram, D. K.; Soncrant, T. T. In *New Concepts of a Blood-Brain Barrier*; Greenwood J. *et al.*, Eds.; Plenum: New York, **1995**, pp. 251-264.

[19] Ecker, G.; Noe, C.R. *Curr. Med. Chem.,* **2004**, *11*, 763.

[20] Clark, D.E. *Drug Discov. Today*, **2003**, *8*, 927.

[21] Norinder, U.; Haeberlein, M. *Adv. Drug Deliv. Rev.,* **2002**, *54*, 291.

[22] Clark, D.E. *Comb. Chem. High Throughput Screen,* **2001**, *4*, 477.

[23] Tamai, I.; Tsuji, A. *J. Pharm. Sci.,* **2000**, *89*, 1371.

[24] Sun, H.; Dai, H.; Shaik, N.; Elmquist, W.F. *Adv. Drug Deliv. Rev.,* **2003**, *55*, 83.

[25] Sai, Y.; Tsuji, A. *Drug Discov. Today*, **2004**, *9*, 712.

[26] Fromm, F.M. *Trends Pharmacol. Sci.,* **2004**, *25*, 423.

[27] Begley, D. and Brightman, M.W. In *Structural and Functional Aspects of the Blood-Brain Barrier; Progress in Drug Research,* Vol. *61*, Prokai, L. and Prokai-Tatrai, K, Eds.; Birkhauser Verlag, Basel, Switzerland, **2003**, pp. 39-78.

[28] Begley, D.J. *Curr. Pharm. Design,* **2004**, *10*, 1295.

[29] Atkinson, F.; Cole, S.; Green, C.; van de Waterbeemd, H. *Curr. Med. Chem.-Central Nervous System Agents,* **2002**, *2*, 229.

[30] Feng, M.R. *Curr. Drug Metab.,* **2002**, *3*, 647.

[31] Sippl, W. *Curr. Med. Chem.-Central Nervous System Agents,* **2002**, *2*, 211.

[32] Lee, G.; Dallas, S.; Hong, M.; Bendayan, R. *Pharmacol. Rev.*, **2001**, *53*, 569.

[33] Tsuji, A.; Tamai, I. *Adv. Drug Deliv. Rev.,* **1999**, *36*, 277.

[34] van de Waterbeemd, H.; Smith, D.A.; Jones, B.C. *J. Comput.-Aid. Mol. Des.,* **2001**, *15*, 273.

[35] Martin, I. *Drug Discov. Today*, **2004**, *9*, 161.

[36] Pardridge, W.M. *Drug Discov. Today*, **2004**, *9*, 392.

[37] Crone, C. and Levitt, D.G. In Capillary Permeability to Small Solutes; Handbook of Physiology, Section 2: The Cardiovascular System, Vol 4: Microcirculation, Part1, Renkin, E.M and Michel, C.C. Eds.; American Physiological Society, Maryland, **1984**, pp. 411-466.

[38] Fenstermacher, J.D.; Blasberg, R.G.; Patlak, C.S. *Pharmacol. Ther.,* **1981**, *14*, 217.

[39] Hammarlund-Udenaes, M. *Adv. Drug Deliv. Rev.,* **2000**, *45*, 283.

[40] Sawchuk, R.J.; Elmquist, W.F. *Adv. Drug Deliv. Rev.,* **2000**, *45*, 295.

[41] de Lange, E.C.M.; de Boer, A.G.; Breimer, D. *Adv. Drug Deliv. Rev.,***2000**, *45*, 295.

[42] Pardridge, W.M. *Adv. Drug Deliv. Rev.,* **1995**, *15*, 5.

[43] Cecchellli, R.; Dehouck, B.; Descamps, L.; Fenart, L.; Buee-Scherrer, V.; Duhem, C.; Lundquist, S.; Rentfel, M.; Torpier, G.; Dehouck, M.P. *Adv. Drug Deliv. Rev.,* **1999**, *36*, 165.

[44] Wolburg, H.; Neuhaus, J.; Kniesel, U.; Krau, B.; Schmid, E.V.; Öcalan, M.; Farrell, C.; Risau, W. *J. Cell Sci.,* **1994**, *107*, 1347.

[45] Gumbleton, M.; Audus, K.L. *J. Pharm. Sci.,* **2001**, *90*, 1681.

[46] Terasaki, T.; Ohtsuki, S.; Hori, S.; Takanaga, H.; Nakashima, E.; Hosoya, K. *Drug Discov. Today*, **2003**, *8*, 944.

[47] Garberg, P.; Ball, M.; Borg, N.; Cecchelli, R.; Fenart, L.; Hurst, R.D.; Lindmark, T.; Mabondzo, A.; Nilsson, J.E.; Raub, T.J.; Stanimirovic, D.; Terasaki, T.; Öberg, J.O.; Österberg, T. *Toxicology in vitro,* **2005**, *19*, 299.

[48] Pardridge, W.M.; Triguero, D.; Yang, J.; Cancilla, P.A. *J. Pharmacol. Exp. Ther.,* **1990**, *253*, 884.

[49] Lundquist, S.; Rentfel, M.; Brillault, J.; Fenart, L.; Cecchelli, R; Dehouck, M.P. *Pharm. Res.,* **2002**, *19*, 976.

[50] Seelig, A. *Eur. J. Biochem.,* **1998**, *251*, 252.

[51] Hansen, D.K.; Scott, D.O.; Otis, K.W.; Lunte, S.M. *J. Pharm. Biomed. Anal.,* **2002**, *27*, 945.

[52] Lauer, R.; Bauer, R.; Linz, B.; Pittner, F.; Peschek, G.A.; Ecker, G.; Friedl, P.; Noe, C.R *IL Farmaco,* **2004**, *59*,133.

[53] Eddy, P.E.; Maleef, B.E.; Hart, T.K.; Smith, P.L. *Adv. Drug Deliv. Rev.,* **1997**, *23*, 185.

[54] Dehouck, M.P.; Dehouck, B.; Schluep, C.; Lemaire, M.; Cecchelli, R. *Eur. J. Pharm. Sci.,* **1995**, *3*, 357.

[55] Usanky, H.H.; Sinko, P.J. *Pharm. Res.,* **2003**, *20*, 390.

[56] Saheki, A.; Terasaki, T.; Tamai, I.; Tsuji, A. *Pharm. Res.,***1994**, *11*, 305.

[57] Pardridge, W.M. *Mol. Interv.,* **2003**, *3*, 90.

[58] Mayer, S.E.; Maickel, R.P.; Brodie, B.B. *J. Pharmacol.,* **1959**, *127*, 205.

[59] Hansch, C.; Steward, A.R.; Iwasa, J. *Mol. Pharmacol.,* **1965**, *1*, 87.

[60] Hansch, C.; Leo, A. and Hoekman, D. In *Exploring QSAR-Fundamentals and Applications in Chemistry and Biology;* Heller, S.R., Ed.; American Chemical Society: Washington DC, **1995**, pp. 387-410.

[61] Hansch, C.; Bjorkroth, J.P.; Leo, A. *J. Pharm. Sci.,* **1987**, *76*, 663.

[62] Levin, V.A. *J. Med. Chem.,* **1980**, *23*, 682.

[63] Schinkel, A.H.; Mol, C.A.A.M.; Wagenaar, E.; van Deemter, L.; Smit, J.J.M.; Borst, P. *Eur. J. Cancer,* **1995**, *31A*, 1295.

[64] Lohmann, C.; Huwel, S.; Galla, H.J. *J. Drug Target,* **2002**, *10*, 263.

[65] Begley, D.J. *Pharmacol Therapeut.,* **2004**, *104*, 29.

[66] Trauble, H. *J. Membrane Biol.,* **1971**, *4*, 193.

[67] Fischer, H.; Gottschlich, R.; Seelig, A. *J. Membrane Biol.,* **1998**, *165*, 201.

[68] Kaliszan, R.; Markuszewski, M. *Int. J. Pharm.,* **1996**, *145*, 9.

[69] Agus, D.B.; Gambhir, S.S.; Pardridge, W.M.; Spielholz, C.; Baselga, J.; Vera J.D.W. *J. Clin. Invest.,* **1997**, *100*, 2842.

[70] Cornford, E.M.; Braun, L.D.; Oldendorf, W.H.; Hill, M.A. *Am. J. Physiol.,* **1982**, *243*, C161.

[71] Bodor, N.; Buchwald, P. *Adv. Drug Deliv. Rev.,* **1999**, *36*, 229.

[72] Kaliszan, R.; In *Structure and Retention in Chromatography. A Chemometric Approach;* Ravindranath, B. Ed.; Harwood Academic Publishers, **1997**, Vol. *1*, Chapter 12, pp. 181-202.

[73] Escuder-Gilabert, L.; Molero-Monfort, M.; Villanueva-Camañas, S.; Medina-Hernández, M.J. *J. Chromatogr. B.,* **2004**, *807*, 193.

[74] Kai, J.; Nakamura, K.; Masuda, T.; Ueda, I.; Fujiwara, H. *J. Med. Chem.*, **1996**, *39*, 2621.

[75] Lien, E.J.; Wang, P.H. *J. Pharm. Sci.,* **1980**, *69*, 648.

[76] Shah, M.V.; Audus, K.L.; Borchardt, R.T. *Pharm. Res.,***1989**, *6*, 624.

[77] Chikhale, E.G.; KaYun, N.G.; Burton, P.S.; Borchardt, R.T. *Pharm. Res.,***1994**, *11*, 412.

[78] Abraham, M.H.; Chada, H.S.; Whiting, G.S.; Mitchell, R.C. *J. Pharm. Sci.,* **1994**, *83*, 1085.

[79] Gratton, J.A.; Abraham, M.H.; Bradbury, M.W.; Chada, H.S. *J. Pharm. Pharmacol.,* **1997**, *49*, 1211.

[80] Abraham, M.H.; Chada, H.S.; Martins, F.; Mitchell, R.C.; Bradbury, M.W.; Gratton, J.A. *Pestic. Sci.,* **1999**, *55*, 78.

[81] Abraham, M.H.; Ibrahim, A.; Zissimos, A.M.; Zhao, Y.H.; Comer, J.; Reynolds, D.P. *Drug Discov. Today*, **2002**, *7*, 1056.

[82] Abraham, M.H. *Eur. J. Med. Chem.,* **2004**, *39*, 235.

[83] Habgood, M.D.; Liu, Z.D.; Dehkordi, L.S.; Khodr, H.H.; Abbott, J.; Hider, R.C. *Biochem. Pharmacol.,* **1999**, *57*, 1305.

[84] Pardridge, W.M.; Mietus, L.J. *J. Clin. Invest.,* **1979**, *64*, 145.

[85] Barnes, K.M.; Dickstein, B.; Cutler Jr., G.B.; Fojo, T.; Bates, S.E. *Biochemistry*, **1996**, *35*, 4820.

[86] Liu, X.; Tu, M.; Kelly, R.S.; Chen, C.; Smith, B.J. *Drug Metab. Dispos.,* **2004**, *32*, 132.

[87] Ertl, P.; Rohde, B.; Selzer, P. *J. Med. Chem.,* **2000**, *43*, 3714.

[88] Murakami, H.; Takanaga, H.; Matsuo, H.; Ohtani, H.; Sawada, Y. *Am. J. Physiol. Heart Circ. Physiol., 279*, **2000**, H1022.

[89] Deguchi, Y.; Nozawa, K.; Yamada, S.; Yokoyama, Y.; Kimura, R. *J. Pharmacol. Exp. Ther.,* **1997**, *280*, 551.

[90] Kusuhara, H.; Sekine, T.; Utsunomiya-Tate, N.; Tsuda, M.; Kojima, R.; Cha, S.H.; Sugiyama, Y.; Kanai, Y.; Endou, H. *J. Biol.. Chem.,* **1999**, *274*, 13675.

[91] Kido, Y.; Tamai, I.; Okamoto, M.; Suzuki, F.; Tsuji, A. *Pharm. Res.,***2000**, *17*, 55.

[92] Gibbs, J.P.; Adeyeye, M.C.; Yang, Z.; Shen, D.D. *Epilepsy Res.,* **2004**, *58*, 53.

[93] Löscher, W.; Potschka, H. *J. Pharmacol. Exp. Ther.,* **2002**, *301*, 7.

[94] Luco, J.M., Salinas, A.P.; Torriero, A.A.; Nieto, R.; Raba, J.; Marchevsky, E. *J. Chem. Inf. Comput. Sci.,* **2003**, *43*, 2129.
[95] Taillardat-Bertschinger, A.; Carrupt, P.A.; Barbato, F.; Testa, B. *J. Med. Chem.,* **2003**, *46*, 1.
[96] Reichel, A.; Begley, D.J. *Pharm. Res.,***1998**, *15*, 1270.
[97] Salminen, T.; Pulli, A.; Taskinen, J. *J. Pharmaceut. Biomed. Anal.,* **1997**, *15*, 469.
[98] Ducarme, A.; Neuwels, M.; Goldstein, S.; Massingham, R. *Eur. J. Med. Chem.,* **1998**, *33*, 215.
[99] Young, R.C.; Mitchell, R.C.; Brown, T.H.; Ganellin, R.C.; Griffihs, R.; Jones, M.; Rana, K.K.; Saunders, D.; Smith, I.R.; Sore, N.E.; Wilks, T.J. *J. Med. Chem.*, **1998**, *31*, 656.
[100] van de Waterbeemd, H.; Kansy, M. *Chimia*, **1992**, *46*, 299.
[101] Calder, J.A.D.; Ganellin, R. *Drug Des. Discov.,* **1994**, *11*, 259.
[102] Abraham, M.H.; Chada, H.S.; Mitchell, R.C. *J. Pharm. Sci.,* **1994**, *83*, 1257.
[103] Abraham, M.H.; Chada, H.S.; Mitchell, R.C. *Drug Des. Discov.,* **1995**, *13*, 123.
[104] Lombardo, F.; Blake, J.F.; Curatolo, W.J. *J. Med. Chem.,* **1996**, *39*, 4750.
[105] Norinder, U.; Sjöberg P.; Österberg, T. *J. Pharm. Sci.,* **1998**, *87*, 952.
[106] Luco, J.M. *J. Chem. Inf. Comput. Sci.,* **1999**, *39*, 396.
[107] Clark, D.E. *J. Pharm. Sci.,* **1999**, *88*, 815.
[108] Kelder, J.; Grootenhuis, P.D.J.; Bayada, D.M.; Delbressine, L.P.C.; Ploemen, J.P. *Pharm. Res.,* **1999**, *16*, 1514.
[109] Segarra, V. ; López, M.; Ryder, H.; Palacios, J.M. *Quant. Struct.-Act. Relat.,* **1997**, *16*, 107.
[110] Feher, M.; Sourial, E.; Schmidt, J.M. *Int. J. Pharm.,* **2000**, *201*, 239.
[111] Österberg, T.; Norinder, U. *J. Chem. Inf. Comput. Sci.,* **2000**, *40*, 1408.
[112] Keresü, G.M.; Molnár, L. *J. Chem. Inf. Comput. Sci.,* **2001**, *41*, 120.
[113] Platts, J.A.; Abraham, M.H.; Zhao, Y.H.; Hersey, A.; Ijaz, L.; Butina, D. *Eur. J. Med. Chem.,* **2001**, *36*, 719.
[114] Liu, R.; Sun, H.; So, S.S. *J. Chem. Inf. Comput. Sci.,* **2001**, *41*, 1623.
[115] Jorgensen, F.S.; Jensen, L.H.; Capion, D.; Christensen, I.T. In *Rational Approaches to Drug Design;* Höltje, H.D. and Sippl, W., Eds.; Prous Science, Barcelona, **2001**, pp. 281-285.
[116] Klamt, A.; Eckert, F.; Hornig, M. *J. Comput.-Aid. Mol. Des.,* **2001**, *15*, 355.
[117] Kaznessis, Y.N.; Snow, M.E.; Blankley, J. *J. Comput.-Aid. Mol. Des.,* **2001**, *15*, 697.
[118] Rose, K.; Hall, L.H. *J. Chem. Inf. Comput. Sci.,* **2002**, *42*, 651.
[119] Ooms, F.; Weber, P.; Carrupt, P.A.; Testa, B. *Biochim. Biophys. Acta,* **2002**, *1587*, 118.
[120] Iyer, M.; Mishra, R.; Hopfinger, A.J. *Pharm. Res.,***2002**, *19*, 1611.
[121] Lobell, M.; Molnár, L.; Keserü, G.M. *J. Pharm. Sci.,***2003**, *92*, 360.
[122] Hutter, M.C. *J. Comput.-Aid. Mol. Des.,* **2003**, *17*, 415.
[123] Subramanian, G.; Kitchen, D.B. *J. Comput.-Aid. Mol. Des.,* **2003**, *17*, 643.
[124] Hou, T.J.; Xu, X.J. *J. Chem. Inf. Comput. Sci.,* **2003**, *43*, 2137.
[125] Stanton, D.T.; Mattioni, B.E.; Knittel, J.J.; Jurs, P.C. *J. Chem. Inf. Comput. Sci.,* **2004**, *44*, 1010.
[126] Sun, H. J. *Chem. Inf. Comput. Sci.,* **2004**, *44*, 748.
[127] Cabrera, M.A.; Bermejo, M.; Pérez, M.; Ramos, R. *J. Pharm. Sci.,* **2004**, *93*, 1701.
[128] Estrada, E.; Uriarte, E. *Curr. Med. Chem.,* **2001**, *8*, 1573.
[129] Pan. D.; Iyer, M.; Liu, J.; Hopfinger, A.J. *J. Chem. Inf. Comput. Sci.,* **2004**, *44*, 2083.
[130] Winkler, D.A.; Burden, F.R. *J. Mol. Graph. Mod.,* **2004**, *22*, 499.
[131] Winkler, D.A.; Burden, F.R. *Drug Discov. Today: Biosilico*, **2004**, *2*, 104.
[132] Dorronsoro, I.; Chana, A.; Abasolo, M.A.; Castro, A.; Gil, C.; Stud, M. *Quant. Struct.-Act. Relat. Comb. Sci.,* **2004**, *23*, 89.
[133] Fu, X.C.; Wang, G.P.; Liang, W.Q.; Yu, Q.S. *Pharmazie*, **2004**, *59*, 126.
[134] Péhourcq, F.; Matoga, M.; Bannwarth, B. *Fund. Clin. Pharmacol.,* **2004**, *18*, 65.
[135] Zah, J.; Terre'Blanche, G.; Erasmus, E.; Malan, S.F. *Bioorg. Med. Chem.,* **2003**, *11*, 3569.
[136] Seelig, A.; Gottschlich, R.; Devant, R.M. *Proc. Natl. Acad. Sci.,* **1994**, *91*, 68.
[137] Suomalainen, P.; Johans, C.; Söderlund, T.; Kinnunen, K.J. *J. Med. Chem.,* **2004**, *47*, 1783.
[138] van de Waterbeemd, H.; Camenisch, G.; Folkers, G.; Chretien, J.R.; Raevsky, O.A. *J. Drug Target*, **1998**, *6*, 151.
[139] Di, L.; Kerns, E.H.; Fan, K.; McConnell, O.J.; Guy, T.C. *Eur. J. Med. Chem.,* **2003**, *38*, 223.
[140] Kansy, M.; Senner, F.; Gubernatur, K. *J. Med. Chem.,* **1998**, *41*, 1007.
[141] Gulyaeva, N.; Zaslavsky, A.; Lechner, P.; Chlenov, M.; McConnell, O.; Chait, A.; Kipnis, V.; Zaslavsky, B. *Eur. J. Med. Chem.,* **2003**, *38*, 391.
[142] Doan, K.M.M.; Humphreys, J.E.; Webster, L.O.; Wring, S.A.; Shampine, L.J.; Serabjit-Singh, C.J.; Adkison, K.K.; Polli, J.W. *J. Pharmacol. Exp. Ther.,* **2002**, *303*, 1029.
[143] Basak, S.C.; Gute, B.D.; Drewes, L.R. *Pharm. Res.,***1996**, *13*, 775.
[144] Cabrera Pérez, M.A.; Sanz, M.B. *Bioorg. Med. Chem.,* **2004**, *12*, 5833.
[145] Crivori, P.; Cruciani, G.; Carrupt, P.A.; Testa, B. *J. Med. Chem.,* **2000**, *43*, 2204.
[146] Wolohan, P.R.N.; Clark, R.D. *J. Comput.-Aid. Mol. Des.,* **2003**, *17*, 65.
[147] Ajay; Bemis, G.W.; Murcko, M.A. *J. Med. Chem.,* **1999**, *42*, 4942.
[148] Keserü, G.M.; Molnár, L.; Greiner, I. *Comb. Chem. High Throughput Screen*, **2000**, *3*, 535.
[149] Doniger, S.; Hofmann, T.; Yeh, J. *J. Comput. Biol.,* **2002**, *9*, 849.
[150] Engkvist, O.; Wrede, P.; Rester, U. *J. Chem. Inf. Comput. Sci.,* **2003**, *43*, 155.
[151] Adenot, M.; Lahana, R. *J. Chem. Inf. Comput. Sci.,* **2004**, *44*, 239.
[152] Doran, A.; Obach, R.S.; Smith, B.J.; Hosea, N.A.; Becker, S.; Callegari, E.; Chen, C.; Chen, X.; Choo, E.; Cianfrogna, J.; Cox, L.M.; Gibbs, J.P.; Gibbs, M.A.; Hatch, H.; Hop, C.E.C.A.; Kasman, I.N.; LaPerle, J.; Liu, J.H.; Liu, X.; Logman, M.; Maclin, D.; Nedza, F.M.; Nelson, F.; Olson, E.; Rahematpura, S.; Raunig, D.; Rogers, S.; Schmidt, K.; Spracklin, D.K.; Szewc, M.; Troutman, M.; Tseng, E.; Tu, M.; Van Deusen, J.W.; Venkatakrishnan, K.; Walens, G.; Wang E.Q.; Wong, D.; Yasgar, A.S.; Zhang C. *Drug Metab. Dispos.,* **2005**, *33*, 165.
[153] Schinkel, A.H.; Wagenaar, E.; Mol, C.A.A.M.; van Deemter, L. *J. Clin. Invest.,* **1996**, *97*, 2517.
[154] Krishna, R.; Mayer, L.D. *Curr. Med. Chem.-Anti-Cancer Agents,* **2001**, *1*, 163.
[155] Wiese, M.; Pajeva, I.K. *Curr. Med. Chem.,* **2001**, *8*, 685.
[156] Stouch, T.R.; Gudmundsson, O. *Adv. Drug Deliv. Rev.,* **2002**, *54*, 315.
[157] Zhang, E.Y.; Phelps, M.A.; Cheng, C.; Ekins, S.; Swaan, P.W. *Adv. Drug Deliv. Rev.,* **2002**, *54*, 329.
[158] Teodori, E.; Dei, S.; Scapecchi, S.; Gualtieri, F. *IL Farmaco,* **2002**, *57*, 385.
[159] Wang, R.B., Kuo, C.L.; Lien, L.L.; Lien, E.J. *J. Clin. Pharm. Ther.,* **2003**, *28*, 203.
[160] Robert, J.; Jarry, C. *J. Med. Chem.,* **2003**, *46*, 1.
[161] http://homeapage.smc.edu/godsil_bill/Lectures/Lecture%202.ppt

Received: March 15, 2005 **Revised: June 15, 2005** **Accepted: July 13, 2005**